One-way operators, absorbing boundary conditions and domain decomposition for wave propagation

Laurence HALPERN

and

Adib RAHMOUNI

Département de Mathématiques, Institut Galilée
Université Paris 13
93430 Villetaneuse
France

Abstract

We present the notion of paraxial operators and applications to absorbing boundary conditions and domain decomposition for hyperbolic problems. We also describe the new concept of perfectly matched layers.

1 Introduction

We treat here the question of computing the solution of a problem in a large, possibly infinite, domain. The applications are numerous: geophysics, aeronautics, oceanography ... The tool for large problems is domain decomposition, where different problems with different scales and/or different numerical discretization methods can be used in different subdomains. Many of these problems are also posed in infinite domains. In some cases the equation in the domain is replaced by a simpler one which for instance represents the propagation in a preferred direction: this leads to the notion of paraxial equations. In any case, the computational domain has to be bounded in all directions. One has to introduce fictitious boundaries with so-called absorbing or farfield boundary conditions. There is a strong connection between these notions, as a transparent boundary operator is a paraxial operator, as we shall demonstrate here. We shall also demonstrate that the optimal transmission condition between two subdomains in domain decomposition is produced by the paraxial operator. This will provide the link between these three notions.

The guiding line here is the notion of wave propagation. In Section 2 we start with the transport equation, where we introduce the notions of finite speed of propagation, well-posedness, numerical schemes, and the necessity of adding extra boundary conditions. In Section 3 we turn to the one-dimensional wave equation, where we introduce the concepts of paraxial operators, absorbing boundary conditions and optimal transmission conditions for domain decomposition. A numerical scheme is described, and a domain decomposition procedure is applied to heterogeneous media. In Section 4 we give precise definitions for the three notions for the wave equation in two dimensions, and we highlight the links between

them. We give some preliminary results on domain decomposition with optimal transmission conditions in this case.

In the last five years, there has been a tremendous activity about a new notion of perfectly matched layers, which is very competitive to absorbing boundary conditions for linear constant coefficient hyperbolic models. Therefore the last section is devoted to the description of this notion, and several improvements.

All the references are to be found in the body of the text.

Contents

2 The one-dimensional transport equation

2.1 The continuous problem

Let us consider the scalar transport equation

$$\frac{\partial u}{\partial t} + a(x)\frac{\partial u}{\partial x} = f \quad \text{on} \quad \mathbb{R} \times (0,T), \tag{2.1}$$

where a is a continuous function of x with a definite sign: a is either positive or negative in the domain. We can write (2.1) as

$$\frac{d}{dt}u(x(t),t) = f(x(t),t), \tag{2.2}$$

where $x(t)$ is defined as the characteristic curve

$$\frac{dx}{dt} = a. \tag{2.3}$$

This expresses the fact that the solution propagates along the *characteristics curves*. If the velocity a is a constant, they are straight lines as described in Fig. 1.

If a is a constant, there are special solutions of this equation, the *plane waves*. They are given by

$$u(x,t) = e^{i(kx-\omega t)}.$$

Such a function is a solution of the equation if and only if ω and k are related through the *dispersion relation*

$$\omega = ak.$$

For general waves, the function $v_\varphi(k) = \omega/k$ is called the phase velocity. Here the dispersion relation is a linear function of k: the model is *non-dispersive*.

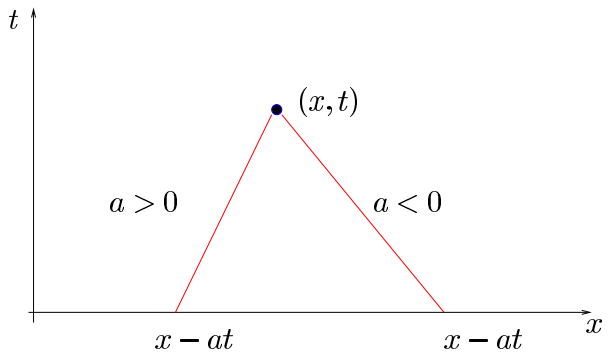

Figure 1: Characteristic lines for a constant velocity a.

2.1.1 The Cauchy problem

We introduce now the *Cauchy problem* by adding initial data

$$u(x,0) = u^{(0)}(x) \quad \text{on} \quad \mathbb{R}. \tag{2.4}$$

We define the *well-posedness* in the sense of Hadamard: a problem is well-posed if

- it has a smooth solution;
- the solution is unique;
- the solution depends continuously on the data.

The following theorem asserts that the Cauchy problem for the transport equation is well-posed:

2.1 Theorem *Assume that the initial velocity $u^{(0)}$ is in $L^2(\mathbb{R})$ and the right-hand side f is in $L^2(0,T;L^2(\mathbb{R}))$. Then problem* (2.1), (2.4) *has a unique solution u in $L^2(0,T;L^2(\mathbb{R}))$. This solution is given on the characteristic curves* (2.3) *by*

$$u(x(t),t) = u^{(0)}(x(0)) + \int_0^t f(x(s),s)\,ds. \tag{2.5}$$

In particular, if a is constant we have

$$u(x,t) = u^{(0)}(x-at) + \int_0^t f(x-a(t-s),s)\,ds.$$

Proof Using (2.2) and the theory of differential equations, a unique characteristic exists through any given point (x,t) and we obtain (2.5). □

This result shows that the solution u at a point (x,t) depends only on the values of the data along the characteristic curve. It proves that *the solution propagates with speed a*: if at time 0 the solution vanishes outside the interval $[\alpha,\beta]$, then at any time t the solution for $f := 0$ vanishes outside the interval $[\alpha + a_* t, \beta + a_* t]$ with $a_* = \sup_{x\in\mathbb{R}} a(x)$.

2.1.2 The initial boundary value problem

We shall suppose here the velocity a to be constant, and introduce the convection equation on the half-line $\mathbb{R}^+$:

$$\frac{\partial u}{\partial t} + a\frac{\partial u}{\partial x} = f \quad \text{in} \quad \mathbb{R}^+ \times (0,T), \tag{2.6}$$

with the initial data

$$u(x,0) = u^0(x) \quad \text{in} \quad \mathbb{R}^+. \tag{2.7}$$

If a is negative, the characteristics leave the domain, the solution travels to the left, so we do not need a condition on the boundary $x = 0$. In the case where a is positive, the characteristics enter the domain, the solution travels to the right, so we need a boundary condition at $x = 0$. This is illustrated in Fig. 2.

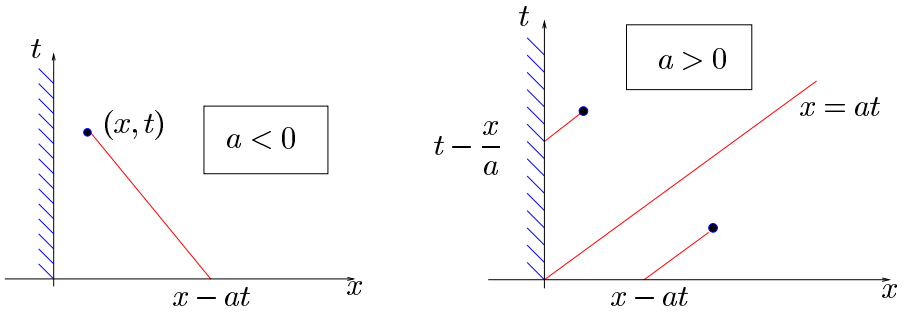

Figure 2: Propagation on the half-line.

The simplest boundary condition is to prescribe the solution on the boundary, that is,

$$u(0,t) = g(t) \quad \text{on} \quad (0,T), \tag{2.8}$$

and the related *initial boundary value problem* is well-posed:

2.2 Theorem *If a is negative, Problem* (2.6), (2.7) *admits a unique solution*

$$u(x,t) = u^0(x - at).$$

If a is positive, Problem (2.6), (2.7) *with boundary condition* (2.8) *has a unique solution*

$$u(x,t) = \begin{cases} u^0(x-at) & \text{for } x > at, \\ g(t - x/a) & \text{for } x < at. \end{cases}$$

The initial boundary value problem is well-posed in $L^2(0,T;L^2(\mathbb{R}_+))$. Furthermore, if the compatibility condition

$$u^0(0) = g(0)$$

is satisfied, then it is well-posed in the space of continuous functions.

2.2 The discrete algorithm

We are given a mesh in time and space, with size Δt and Δx; the mesh points in space are $x_j = j\Delta x$, and in time they are $t^n = n\Delta t$. As usual we denote by u_j^n an approximation of $u(x_j, t^n)$.

2.2.1 Examples

The simplest scheme is the upwind scheme (Fig. 3) given by

$$\frac{u_j^{n+1} - u_j^n}{\Delta t} + a\frac{u_j^n - u_{j-1}^n}{\Delta x} = 0. \tag{2.9}$$

It is of order one in time and in space. For a better accuracy in time and space, the leap-frog scheme is very classical (Fig. 4). It is of order 2 in time and space, but it is centered, which can alter the dispersion properties,

$$\frac{u_j^{n+1} - u_j^{n-1}}{2\Delta t} + a\frac{u_{j+1}^n - u_{j-1}^n}{2\Delta x} = 0. \tag{2.10}$$

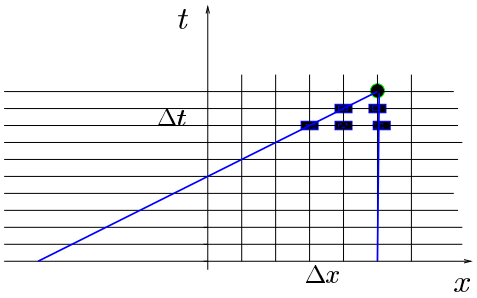

Figure 3: Upwind scheme (2.9).

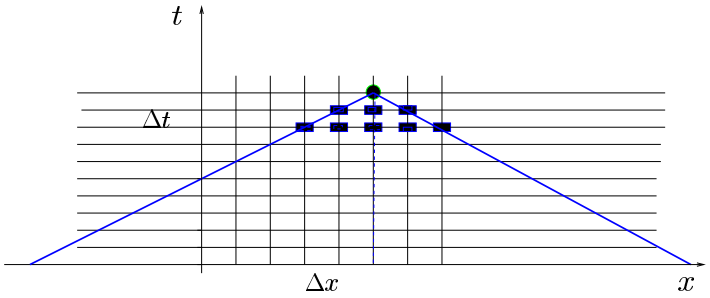

Figure 4: Leap-frog scheme (2.10).

2.2.2 The Cauchy problem. Propagation, stability, convergence

In Fig. 5, the solid line represents the numerical cone of dependence for the upwind scheme (2.9), while the dashed lined represents the characteristic line. Taking an initial value vanishing at every point but one on the grid shows that in the case where a is larger than $\Delta x/\Delta t$, the scheme cannot converge.

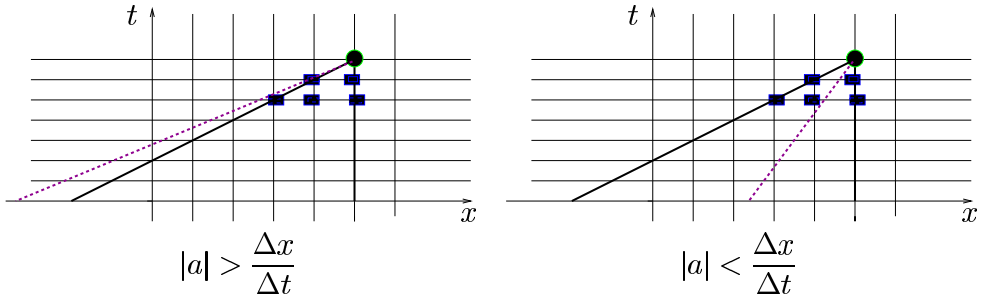

Figure 5: Cone of dependence for the upwind scheme (2.9) (dashed) together with the characteristic line for the equation (solid).

So we have the following:

2.3 Theorem *If a three-points numerical scheme converges, then the following CFL condition holds :*

$$\gamma = |a|\frac{\Delta t}{\Delta x} \leq 1. \tag{2.11}$$

Here CFL is the classical shorthand for the three mathematicians Courant-Friedrichs-Lewy [35]. As for stability, we have the following definition. We shall call u_h^n the sequence $(u_j^n)_{j\in\mathbb{R}}$.

2.4 Definition The scheme is *stable* if there exists a real number α such that, for every meshsize in time Δt, and space Δx, we have, for any time step n, that

$$\|u_h^n\|_{l^2} \leq Ce^{\alpha n\Delta t}\|u_h^0\|_{l^2}.$$

A simple characterization is given by a discrete Fourier transform in space: for any real number χ we consider simple waves of the type

$$u_j^n = \hat{u}^n e^{i\chi x_j}. \tag{2.12}$$

Inserting (2.12) into the scheme, we get for a one step method in time

$$\hat{u}^{n+1} = g(\gamma, \chi\Delta x)\hat{u}^n. \tag{2.13}$$

The function g is the amplification factor, and as (2.13) suggests, it depends only on two quantities, γ and $\chi\Delta x$. For the upwind scheme (2.9), for instance, we have

$$g(\gamma, \zeta) = 1 - \gamma(1 - e^{-i\zeta}).$$

For a second order scheme like the leapfrog scheme (2.10), there is an amplification matrix

$$\begin{pmatrix} \hat{u}^{n+1} \\ \hat{u}^n \end{pmatrix} = G(\gamma, \chi\Delta x)\begin{pmatrix} \hat{u}^n \\ \hat{u}^{n-1} \end{pmatrix}.$$

For instance, for the leapfrog scheme we have

$$G(\gamma, \zeta) = \begin{pmatrix} 1 & -2i\gamma\sin\zeta \\ 1 & 0 \end{pmatrix}.$$

Then the scheme is stable for step sizes Δt and Δx if and only if there exists a real number β such that for any ζ we have

$$\|G(\gamma,\zeta)\| \leq e^{\beta\Delta t},$$

where $\|\cdot\|$ is the usual euclidian norm on the space of matrices. This leads to a condition on γ. For instance, for the two schemes above, the scheme is stable under the strict CFL condition. If we go to higher orders in time and space, the stability condition becomes more restrictive. For details on these notions see [35].

Stability and consistency (i.e. order greater than one) are the key notions for a *linear scheme*, due to the Lax theorem:

$$\textit{Stability} \ + \ \textit{consistency} \iff \textit{convergence}.$$

2.2.3 The initial boundary value problem

We consider a scheme with homogeneous data and initial values, and a discrete inhomogeneous boundary condition.

We insert $u_j^n = \alpha z^n r^j$ into the homogeneous equation. Then we get the dispersion relation between z and r, which we solve as an equation in the variable r as a function of z. We now insert u_j^n into the heterogeneous boundary condition. We get an equation like $E(z,\gamma)\alpha = g$. If the preceding equation is invertible for all z such that $|z| \geq 1$, it is called *GKS stable* (for Gustafsson, Kreiss and Sundström). These notions of stability are explained in detail in the book by Strikwerda [35].

This notion of stability is stronger than the usual L^2 stability, because it implies estimates on the boundary. Some boundary conditions can be L^2 stable, but not GKS stable. The strength of the condition comes from the fact that it provides the algebraic criterium cited above.

2.2.4 Transparent boundary conditions

We suppose here that $a > 0$, and we consider the problem on the half-line $x > 0$, with a boundary condition $g(t)$ at $x = 0$. Suppose we want to compute the solution only on the *domain of interest* $]0, A[$. Since the solution propagates to the right, Theorem 2.2 gives the answer : we do not need any information on the boundary. We introduce now a discretized problem. Suppose it is the upwind scheme (2.9). Fig. 6 shows that we do not need any information on the boundary $x = A$ either.

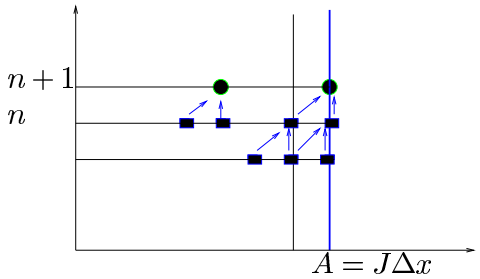

Figure 6: Upwind scheme (2.9) on a right boundary.

The situation is totally different if we deal with centered schemes, as illustrated in Fig. 7:

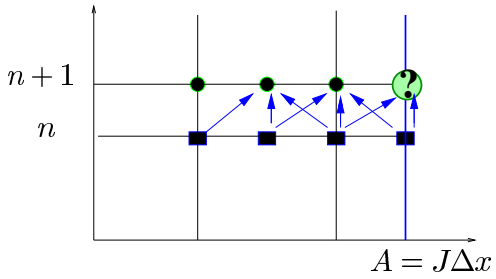

Figure 7: Leap-frog scheme (2.10) on the right boundary.

At time $n+1$, we do not have enough information to compute u_J^{n+1}. The usual procedures are either to use an upwind scheme on the boundary, to extrapolate, or to create fictitious points outside the domain [18]. The constraints are the stability of the discrete initial boundary value problem, and the consistency with the equation. Apart from the important work by B. Gustafsson in [18] on the stability, we do not know of a general analysis of this problem.

3 The one-dimensional wave equation

3.1 The homogeneous case

Consider the one-dimensional wave equation with a constant velocity c:

$$\frac{1}{c^2}\frac{\partial^2 u}{\partial t^2} - \frac{\partial^2 u}{\partial x^2} = f \quad \text{in} \quad \mathbb{R}\times(0,T). \tag{3.1}$$

3.1.1 Propagation properties

If the right-hand side vanishes, $f = 0$, the general solution is given by

$$u(x,t) = F(x+ct) + G(x-ct), \tag{3.2}$$

where F and G are arbitrary functions. The first term $(x,t) \mapsto F(x+ct)$ propagates to the left, along the characteristics with slope $-c$:

$$\left(\frac{1}{c}\frac{\partial}{\partial t} - \frac{\partial}{\partial x}\right) F(x+ct) = 0, \tag{3.3}$$

while the second term $(x,t) \mapsto G(x-ct)$ propagates to the right, along the characteristics with slope $+c$:

$$\left(\frac{1}{c}\frac{\partial}{\partial t} + \frac{\partial}{\partial x}\right) G(x-ct) = 0. \tag{3.4}$$

Let us now introduce the plane waves

$$u(x,t) = e^{i(kx-\omega t)}.$$

The dispersion relation is given by

$$\omega^2 = c^2 k^2.$$

3.1.2 The Cauchy problem

We now add initial data, given by an initial displacement and an initial velocity,

$$u(x,0) = u^{(0)}(x), \qquad \frac{\partial u}{\partial t}(x,0) = u^{(1)}(x) \tag{3.5}$$

The solution of (3.1), (3.5) can be given explicitely by the d'Alembert formula (3.6),

$$\boxed{\begin{aligned} u(x,t) = \frac{1}{2}[u^{(0)}(x+ct) + u^{(0)}(x-ct)] \\ + \frac{1}{2c}\int_{x-ct}^{x+ct} u^{(1)}(\zeta)\,d\zeta + \frac{c}{2}\iint_{\mathcal{C}_{x,t}} f(\zeta,\tau)\,d\zeta\,d\tau. \end{aligned}} \tag{3.6}$$

Fig. 8 represents the cone of dependence for the solution. It shows that the solution at time t and point x depends only on the data in the cone $\mathcal{C}_{x,t}$.

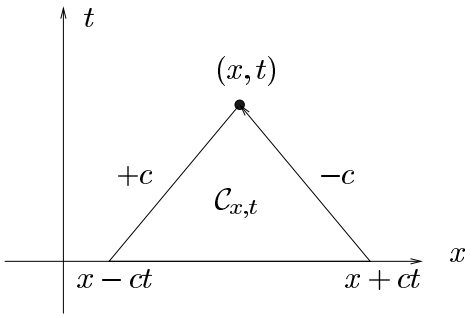

Figure 8: Cone of dependence for point (x,t).

Fig. 9 illustrates the propagation for zero right-hand side f and $u^{(1)}$, and initial values given by a gaussian function

$$u^{(0)}(x) = e^{-x^2} \tag{3.7}$$

The velocity is equal to 1. In the beginning the signal splits, and then each part goes its own way.

A direct consequence of the d'Alembert formula (3.6) is the

3.1 Theorem *The solution of the wave equation propagates with speed c: if the initial data vanish outside* $[a,b]$, *for any time* t *the solution* $u(.,t)$ *vanishes outside* $[a-ct, b+ct]$.

An illustration is given by the domain of influence $\mathcal{D}$ in Fig. 10.

3.1.3 The initial boundary value problem

We consider the wave equation on the half-line $(X, +\infty[$ with initial values $u^{(0)}$ and $u^{(1)}$ and vanishing right-hand side. The diagram in Fig. 11 is very illuminating. It shows the modified cone of dependence.

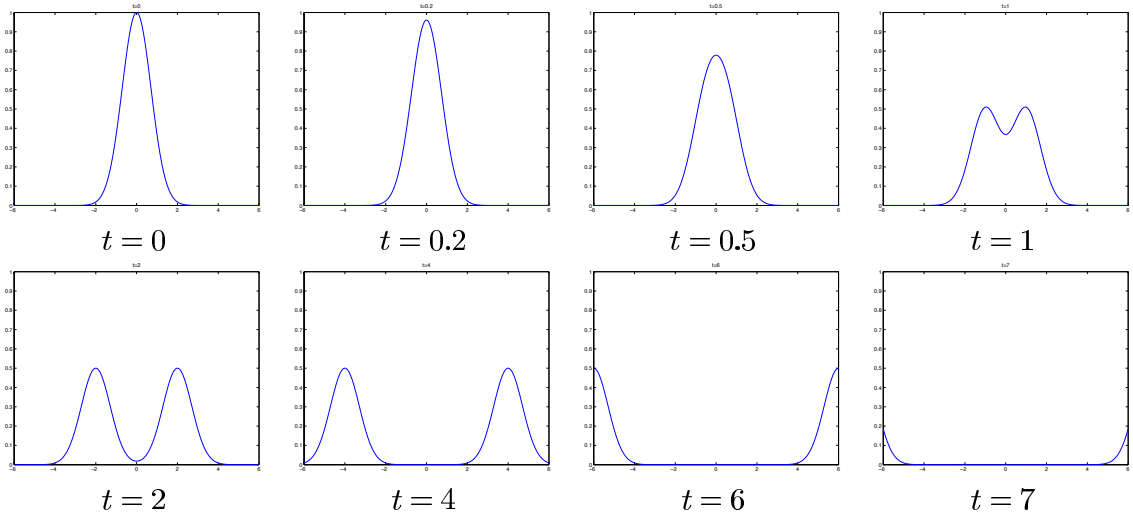

Figure 9: Evolution of the data (3.7).

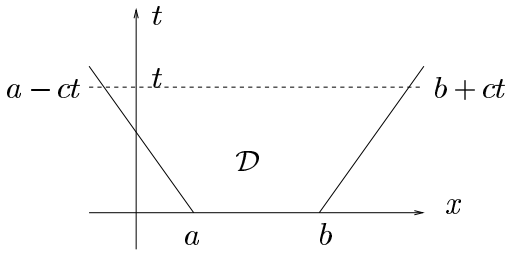

Figure 10: Domain of influence.

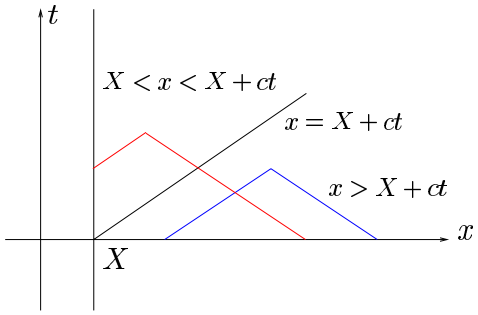

Figure 11: Domain of dependence for the problem on $(X, +\infty[$.

As in the case of the transport equation, the need for a boundary condition appears clearly. It is given for instance by an *inhomogeneous Dirichlet boundary condition* at $x = X$, which amounts to fixing the displacement of the rope at the extremity,

$$u(X,t) = g(t) \quad \text{for} \quad t \in (0,T).$$

The initial boundary value problem is given by

$$\begin{cases} \dfrac{1}{c^2}\dfrac{\partial^2 u}{\partial t^2} - \dfrac{\partial^2 u}{\partial x^2} = 0 \quad \text{in} \quad (X, +\infty) \times (0, T), \\ u(\cdot, 0) = u^{(0)}, \quad \dfrac{\partial u}{\partial t}(\cdot, 0) = u^{(1)} \quad \text{on} \quad (X, +\infty), \\ u(X, t) = g(t) \quad \text{for} \quad t \in (0, T). \end{cases} \tag{3.8}$$

3.2 Theorem *Problem* (3.8) *has a unique solution given by the formula*

$$u(x,t) = \begin{cases} \dfrac{1}{2}[u^{(0)}(x+ct) + u^{(0)}(x-ct)] + \dfrac{1}{2c}\displaystyle\int_{x-ct}^{x+ct} u^{(1)}(\zeta)\, d\zeta & \text{if } x - ct > X, \\ \dfrac{1}{2}[u^{(0)}(x+ct) - u^{(0)}(2X - (x-ct))] & \\ \quad + \dfrac{1}{2c}\displaystyle\int_{2X-(x-ct)}^{x+ct} u^{(1)}(\zeta)\, d\zeta + g\left(t + \dfrac{X-x}{c}\right) & \text{if } x - ct < X. \end{cases} \tag{3.9}$$

In Fig. 12 we illustrate the principle of images: the Dirichlet boundary condition plays the role of a mirror.

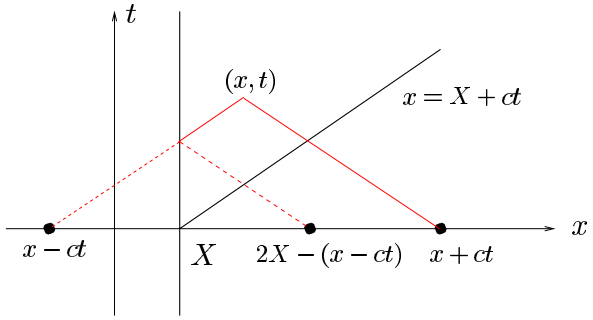

Figure 12: Principle of images on $(X, +\infty)$.

Fig. 13 represents the reflection by a homogeneous Dirichlet boundary condition on the left for the same shape of initial value $u^{(0)}(x) = e^{-3(x-2)^2}$. Of course we can write the same formulae for the problems on $(-\infty, X)$ and (X, Y).

Consider now another boundary condition, which is closely related to domain decomposition and transparent boundary conditions, and will be useful in the sequel. We consider the half-line $(X, +\infty)$, with boundary condition at $x = X$ given by

$$\left(\alpha\frac{\partial u}{\partial t} + \frac{\partial u}{\partial x}\right)(X, t) = g(t). \tag{3.10}$$

In order to make the notations lighter, we shall consider here the initial data to be zero. With the same techniques as before we obtain

$$u(x,t) = F(x+ct) + G(x-ct),$$

with, on the one hand,

$$F'(x) = G'(x) = 0 \quad \text{for all} \quad x > X, \tag{3.11}$$

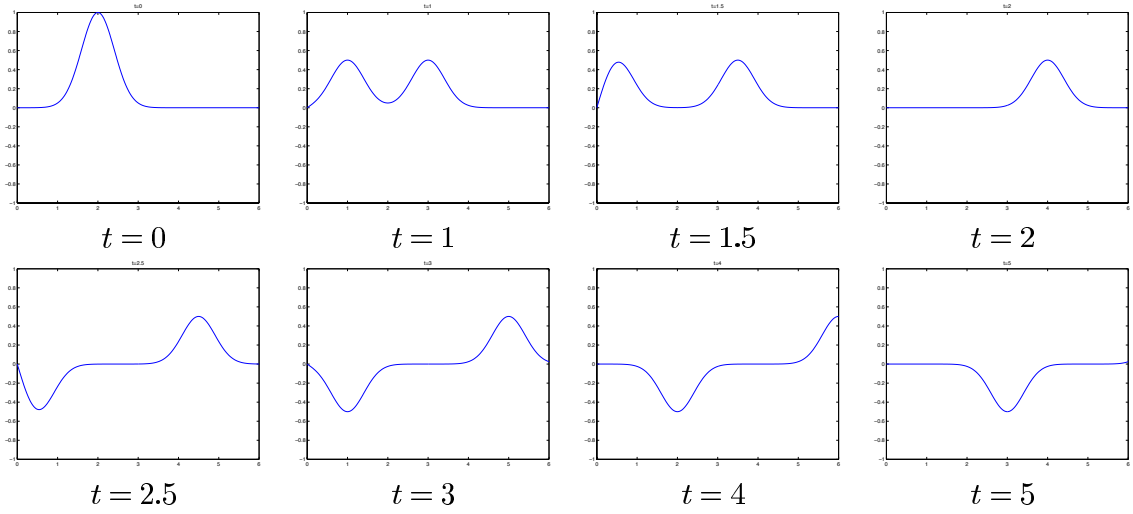

Figure 13: Complete reflection by a Dirichlet boundary condition.

and, on the other hand,

$$(\alpha c + 1)F'(X + ct) + (-\alpha c + 1)G'(X - ct) = g(t) \quad \text{for all} \quad t > 0$$

which by (3.11) gives

$$(-\alpha c + 1)G'(X - ct) = g(t) \quad \text{for all} \quad t > 0.$$

If α is different from $1/c$, this equation can be solved modulo an additive constant :

$$G(x) = \frac{1}{\alpha c - 1} \int_x^X g\left(\frac{X - \eta}{c}\right) d\eta + C \quad \text{for all} \quad x < X.$$

The solution of the initial boundary value problem with boundary condition (3.10) is defined modulo an additive constant C by

$$u(x,t) = \begin{cases} 0, & x - ct > X, \\ \dfrac{1}{\alpha c - 1} \displaystyle\int_{x-ct}^X g\left(\frac{X - \eta}{c}\right) d\eta + C, & x - ct < X. \end{cases}$$

The constant C is determined if we require the solution to be continuous

$$u(x,t) = \begin{cases} 0, & x - ct > X, \\ \dfrac{1}{\alpha c - 1} \displaystyle\int_{x-ct}^X g\left(\frac{X - \eta}{c}\right) d\eta, & x - ct < X. \end{cases}$$

In the same way, the continuous solution of the wave equation on $(-\infty, X)$ with boundary condition at $x = X$ given by

$$\left(\beta \frac{\partial u}{\partial t} + \frac{\partial u}{\partial x}\right)(X,t) = h(t)$$

is

$$u(x,t) = \begin{cases} 0, & x + ct < X, \\ \dfrac{1}{\beta c + 1} \displaystyle\int_X^{x+ct} h\left(\frac{\eta - X}{c}\right) d\eta, & x + ct > X. \end{cases}$$

On an interval (a, b) with boundary conditions

$$\begin{cases} \left(\alpha \dfrac{\partial u}{\partial t} + \dfrac{\partial u}{\partial x}\right)(a,t) = g(t), \\ \left(\beta \dfrac{\partial u}{\partial t} + \dfrac{\partial u}{\partial x}\right)(b,t) = h(t), \end{cases}$$

the continuous solution with zero initial values is

$$u(x,t) = \begin{cases} 0, & x - ct > a \text{ and } x + ct < b, \\ \frac{1}{\alpha c - 1} \int_{x-ct}^{a} g(\frac{a-\eta}{c})\, d\eta, & x - ct < a \text{ and } x + ct < b, \\ \frac{1}{\beta c + 1} \int_{b}^{x+ct} h(\frac{\eta - b}{c})\, d\eta, & x - ct > a \text{ and } x + ct > b, \\ \frac{1}{\alpha c - 1} \int_{x-ct}^{a} g(\frac{a-\eta}{c})\, d\eta + \frac{1}{\beta c + 1} \int_{b}^{x+ct} h(\frac{\eta - b}{c})\, d\eta, & x - ct < a \text{ and } x + ct > b. \end{cases}$$

3.1.4 Transparent boundary condition

Suppose the initial data are compactly supported in (a, b). Due to (3.2)–(3.4), we have

$$\left(\frac{1}{c}\frac{\partial u}{\partial t} - \frac{\partial u}{\partial x}\right)(a,t) = 0, \tag{3.12}$$

$$\left(\frac{1}{c}\frac{\partial u}{\partial t} + \frac{\partial u}{\partial x}\right)(b,t) = 0. \tag{3.13}$$

We now introduce the reflection coefficient. A plane wave propagating to the right is given by $U^I = e^{i\omega(x-ct)}$. For a given boundary condition **BC** at $x = 0$, the reflected wave is $U^R = Re^{i\omega(x+ct)}$ if the sum satisfies the boundary condition **BC**:

$$\mathbf{BC}(U^I + U^R) = 0.$$

Table 1 gives the reflection coefficient for various boundary conditions. It shows that Neumann and Dirichlet are perfectly reflecting, and the transparent boundary condition (3.13) is actually not reflecting at all. It also shows a family of absorbing boundary conditions (i.e. such that the reflection coefficient is smaller than 1) with positive parameter β.

3.1.5 Domain decomposition

For evolution problems, classical methods are based either on explicit schemes, which implies communication at every time step, or on implicit schemes, which gives an elliptic equation to solve at every time step [29, 25]. In both cases it is difficult to use a varying time step for different parts of the domain. However, for the wave equation it is often desirable to choose different time steps in different physical domains. The goals of our strategy are the following: to reduce the communications (and thus the costs), to use non-conformal discretization, and to

Dirichlet boundary condition	$u = 0$	$R = -1$
Neumann boundary condition	$\dfrac{\partial u}{\partial x} = 0$	$R = 1$
Absorbing boundary condition	$\dfrac{\beta}{c}\dfrac{\partial u}{\partial t} + \dfrac{\partial u}{\partial x} = 0$	$R = \dfrac{1-\beta}{1+\beta}$
Transparent boundary condition	$\dfrac{1}{c}\dfrac{\partial u}{\partial t} + \dfrac{\partial u}{\partial x} = 0$	$R = 0$

Table 1: Reflection coefficient for various boundary conditions.

be able to couple different codes. We will build a domain decomposition algorithm such that it works with or without overlap, is global in time, easy to implement, and the convergence is optimal. As we now show, the tool is the transparent boundary condition. For details in this section see [17, 16].

The straightforward extension of the Schwarz algorithm We present the algorithm in the case of two subdomains, $\Omega_1 = (-\infty, L)$ and $\Omega_2 = (0, +\infty)$. At step n, we solve two subproblems in $\Omega_i \times (0,T)$, with Dirichlet data on the boundary given by the previous step in the other domain. The solution in $\Omega_i \times (0,T)$ at step n is called u_i^n. The classical Schwarz algorithm extended to space-time domains is then given by:

$$\left.\begin{array}{l} \left(\dfrac{1}{c^2}\dfrac{\partial^2}{\partial t^2} - \dfrac{\partial^2}{\partial x^2}\right) u_i^n = f \text{ in } \Omega_i \times (0,T) \text{ for } i = 1,2, \\ \text{with initial data for } i = 1,2: \\ u_i^n(.,0) = u^{(0)} \text{ in } \Omega_i, \ \dfrac{\partial u_i^n}{\partial t}(.,0) = u^{(1)} \text{ in } \Omega_i, \\ \text{and transmission conditions:} \\ u_1^n(L,.) = u_2^{n-1}(L,.), \ u_2^n(0,.) = u_1^{n-1}(0,.) \text{ in } (0,T). \end{array}\right\} \tag{3.14}$$

3.3 Theorem *For the straightforward extension* (3.14) *of the Schwarz algorithm, convergence is achieved in a finite number of iterations, $n > Tc/L$.*

Proof The proof can be found in [15], but we describe it here for clarity. Consider the errors $U_i^n = u_i^n - u$. They satisfy the system (3.14) with zero data f and zero initial values. Using formula (3.9), we have

$$\begin{array}{ll} \text{for } x - ct > 0, & U_2^{n+1}(x,t) = 0, \\ \text{for } x - ct < 0, & U_2^{n+1}(x,t) = U_1^n\left(t - \dfrac{x}{c}\right), \end{array} \tag{3.15}$$

and

$$\begin{array}{ll} \text{for } x + ct < L, & U_1^{n+1}(x,t) = 0, \\ \text{for } x + ct > L, & U_1^{n+1}(x,t) = U_2^n\left(t - \dfrac{L-x}{c}\right). \end{array} \tag{3.16}$$

We can draw the diagram in Fig. 14:

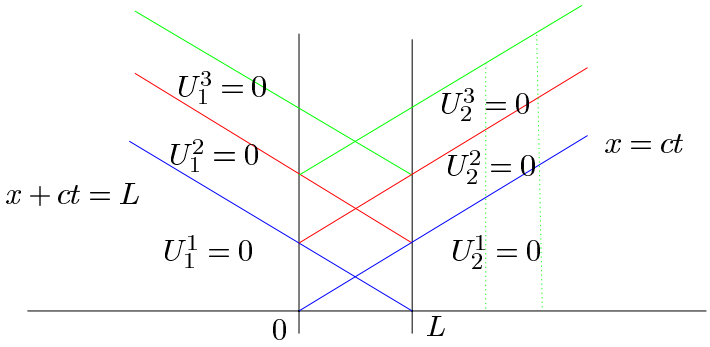

Figure 14: Evolution of the Schwarz algorithm with Dirichlet transmission conditions.

We can now read the end of the proof on Fig. 14 using (3.15) and (3.16). □

We illustrate this behaviour by an example ($c = 1$, $T = 3$). Fig. 15 shows the exact solution, Figs. 16–18 the first five iterates for $L = 0.4$.

Fig. 19 presents the convergence history in this example for two values of the overlap $L = 0.4$ and $L = 0.2$. According to Theorem 3.3, the convergence is achieved for $n > 3/0.4 = 7.5$, resp. $n > 3/0.2 = 15$.

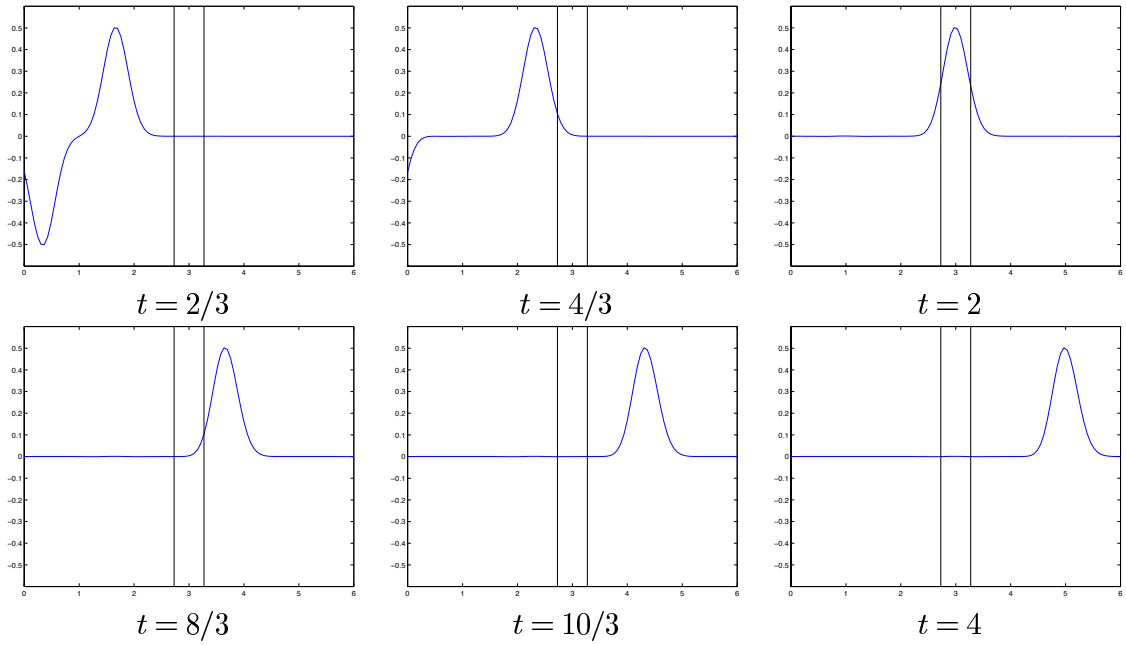

Figure 15: Exact solution.

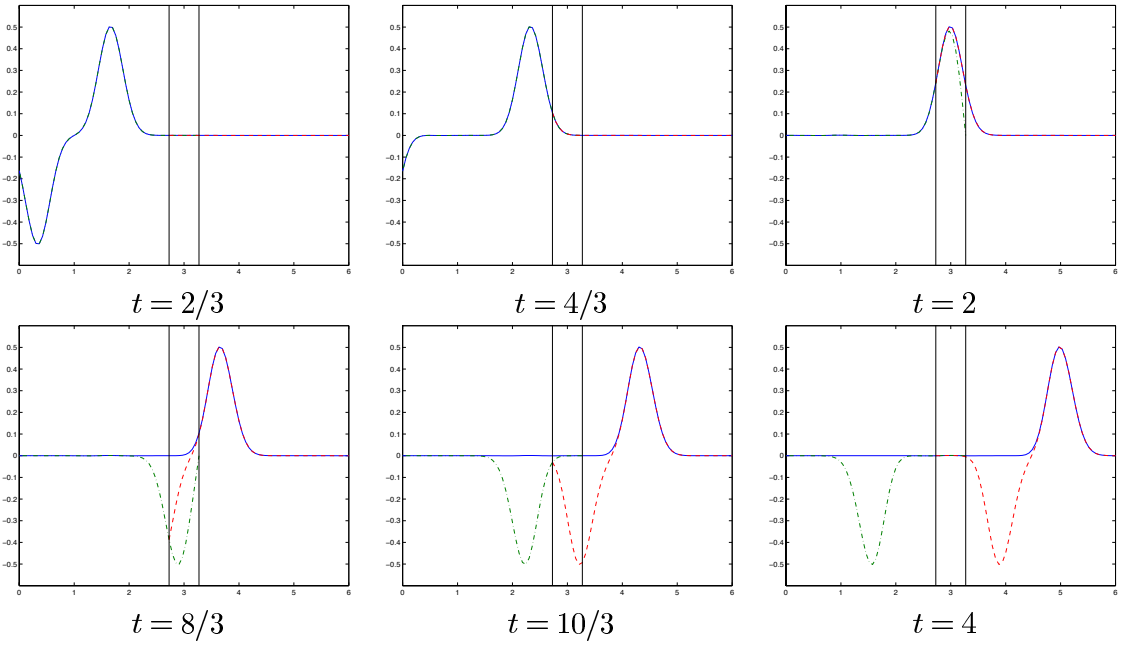

Figure 16: First iteration (dash-dot) u_1^1 and second iteration (dashed) u_2^2 for the Dirichlet transmission conditions together with the exact solution (solid).

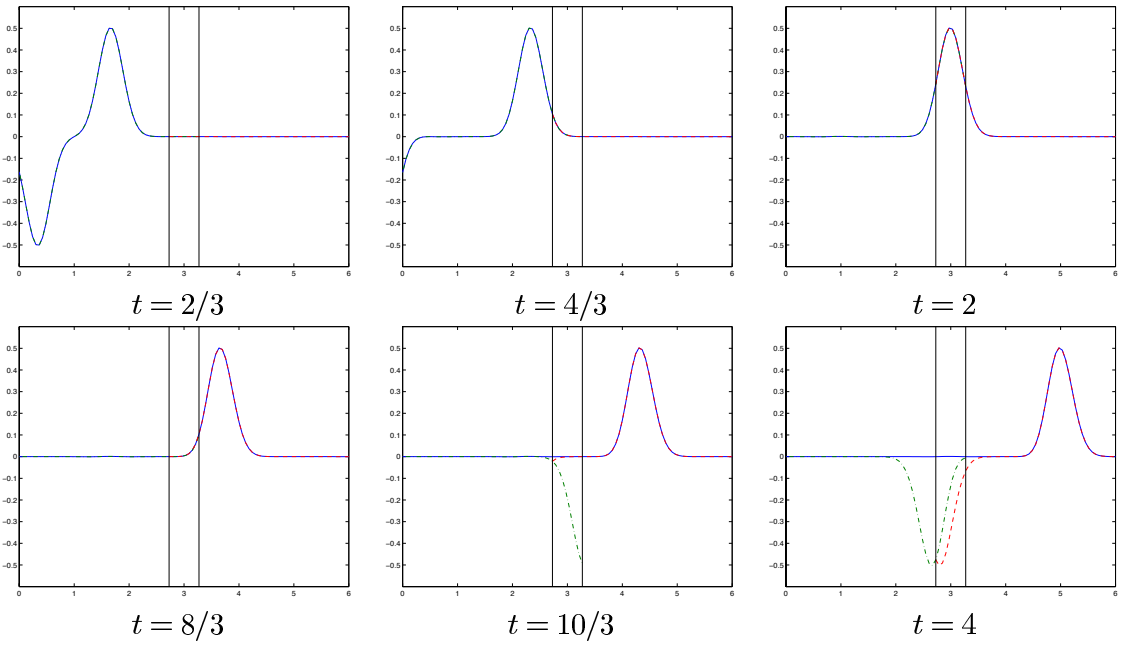

Figure 17: Third iteration (dash-dot) u_1^3 and fourth iteration (dashed) u_2^4 for the Dirichlet transmission conditions together with the exact solution (solid).

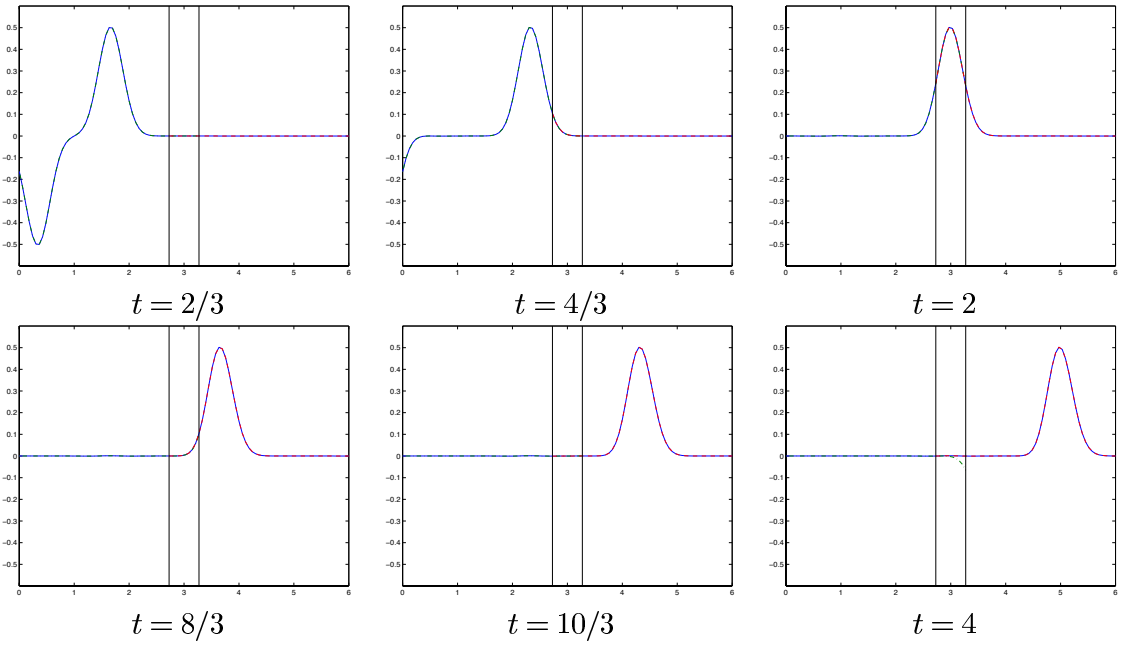

Figure 18: Fifth iteration (dash-dot) u_1^5 and sixth iteration (dashed) u_2^6 for the Dirichlet transmission conditions together with the exact solution (solid).

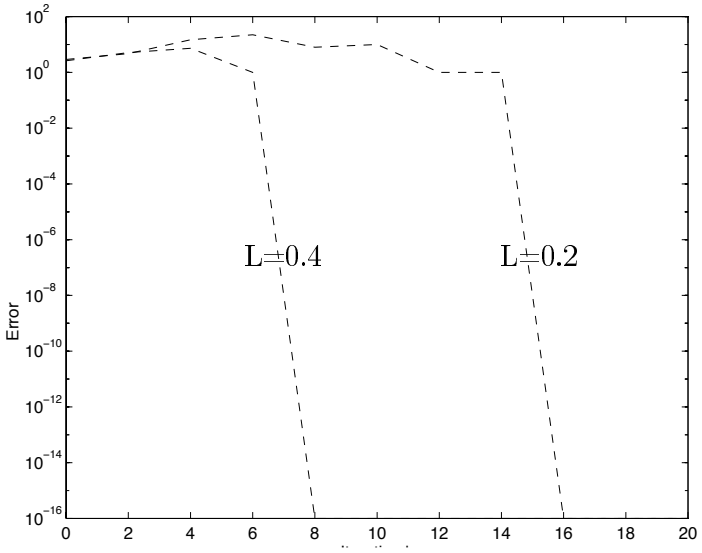

Figure 19: Convergence history for the Schwarz algorithm applied to the wave equation: error versus number of iterations.

3.1.6 The optimal Schwarz algorithm: transparent transmission condition

Note that by (3.15) and (3.16), for any transmission conditions, the error U_1^n on the left is a function of $x-ct$, while the error U_2^n on the right is a function of $x+ct$. This in turn implies the following identities for $n \geq 1$ and any positive time:

$$\begin{cases} \left(\dfrac{\partial}{\partial x} + \dfrac{1}{c}\dfrac{\partial}{\partial t}\right) U_2^n(L,t) = 0, \\ \left(\dfrac{\partial}{\partial x} - \dfrac{1}{c}\dfrac{\partial}{\partial t}\right) U_1^n(0,t) = 0. \end{cases}$$

This observation leads to the following important

3.4 Theorem *The transmission conditions defined by*

$$\left(\frac{\partial}{\partial x} + \frac{1}{c}\frac{\partial}{\partial t}\right) u_1^{n+1}(L,t) = \left(\frac{\partial}{\partial x} + \frac{1}{c}\frac{\partial}{\partial t}\right) u_2^n(L,t),$$
$$\left(\frac{\partial}{\partial x} - \frac{1}{c}\frac{\partial}{\partial t}\right) u_2^{n+1}(0,t) = \left(\frac{\partial}{\partial x} - \frac{1}{c}\frac{\partial}{\partial t}\right) u_1^n(0,t),$$

lead to well-posed initial boundary value problems even without overlap and they are optimal: convergence in the Schwarz algorithm with these transmission conditions is achieved in two iterations, i.e., u_i^2 is identical to u in Ω_i.

An example without overlap The next example shows the convergence to the accuracy of the numerical scheme without overlap. The velocity is $c = 1$, the computation is done on $(0,T)$ with $T = 2$. The initial data are $u(x,0) = 0$, $\partial_t u(x,0) = -100(0.5-x)e^{-50(0.5-x)^2}$. The domain $(0,2)$ is divided into two subdomains $(0,1)$ and $(1,2)$. The initial guess (u_i^0), $i = 1,2$, is naturally chosen to be 0. The scheme is a second order finite volume scheme.

grid	error after 2 iterations	discretization error
50×50	2.6128e − 04	2.1515e − 02
100×100	2.7305e − 05	4.9472e − 03
200×200	3.2361e − 06	1.2218e − 03
400×400	3.9852e − 07	3.0321e − 04
800×800	4.9532e − 08	7.5567e − 05

Table 2: Convergence in two iterations to the accuracy of the numerical scheme.

3.2 The heterogeneous case

We consider now a variable velocity $c(x)$. We suppose c to be positive, and such that there exist two positive real numbers c_* and c^* satisfying

$$c_* \leq c(x) \leq c^*, \quad \text{a.e. in} \quad \mathbb{R}.$$

The wave equation is now

$$\frac{1}{c(x)^2}\frac{\partial^2 u}{\partial t^2} - \frac{\partial^2 u}{\partial x^2} = f \quad \text{in} \quad \mathbb{R} \times (0,T). \tag{3.17}$$

3.2.1 Energy estimates and well-posedness

We first give an existence result in Sobolev spaces :

3.5 Theorem *If $u^{(0)}$ is in $H^1(\mathbb{R})$, $u^{(1)}$ is in $L^2(\mathbb{R})$ and f is in $L^2(0,T;L^2(\mathbb{R}))$, then there exists a unique solution u in $H^1(0,T;L^2(\mathbb{R})) \cap L^2(0,T;H^1(\mathbb{R}))$ to* (3.5), (3.17). *Moreover u is in $\mathcal{C}^0(0,T;L^2(\mathbb{R}))$.*

The complete proof of the theorem is beyond the scope of these lectures. It relies on the use of a finite difference scheme, through *energy estimates*:

3.6 Lemma *Let u be a smooth solution of* (3.17). *Defining the total energy at time t by*

$$\mathcal{E}(t) = \int_{\mathbb{R}} e(x,t)\,dx, \qquad e(x,t) = \frac{1}{2c^2}\left(\frac{\partial u}{\partial t}\right)^2 + \frac{1}{2}\left(\frac{\partial u}{\partial x}\right)^2,$$

we have the energy identity

$$\frac{d}{dt}\mathcal{E}(t) = \int_{\mathbb{R}} f(x,t)\frac{\partial u}{\partial t}\,dx.$$

In particular, without external forces (i.e. $f \equiv 0$), the energy is preserved in time.

In order to obtain the energy, we multiply the equation by $\partial u/\partial t$ and integrate in space on $\mathbb{R}$.

3.7 Remark The solution of the wave equation is in $L^2(0,T)$ for any finite time T but not in $L^2(0,+\infty)$.

3.2.2 Propagation properties

In a heterogeneous medium there is no explicit formula like the d'Alembert formula. However, one can still give a result for the finite speed of propagation:

3.8 Theorem *The solution of* (3.17) *with zero right-hand side propagates with at most the velocity $c^* = \sup_{x\in\mathbb{R}} c(x)$; if the initial conditions vanish outside $[a,b]$, then for any time t the solution vanishes outside $[a - c^*t, b + c^*t]$.*

Proof Let V be a positive real number. We introduce the energy on the moving half-line $(b+Vt, +\infty)$

$$\mathcal{E}_V(t) = \int_{b+Vt}^{+\infty} e(x,t)\,dx.$$

Taking the derivative in time we get

$$\frac{d}{dt}\mathcal{E}_V(t) = \int_{b+Vt}^{+\infty} \frac{\partial}{\partial t} e(x,t)\,dx - Ve(b+Vt,t).$$

We handle the first time by using the equation:

$$\int_{b+Vt}^{+\infty} \frac{\partial}{\partial t} e(x,t)\,dx = \int_{b+Vt}^{+\infty} \left[\frac{1}{c(x)^2}\frac{\partial u}{\partial t}\frac{\partial^2 u}{\partial t^2} + \frac{\partial u}{\partial x}\frac{\partial^2 u}{\partial t \partial x}\right] dx.$$

By Green's formula this transforms to

$$\int_{b+Vt}^{+\infty} \frac{\partial}{\partial t} e(x,t)\,dx = \int_{b+Vt}^{+\infty} \left(\frac{1}{c(x)^2} \frac{\partial^2 u}{\partial t^2} - \frac{\partial^2 u}{\partial x^2} \right) \cdot \frac{\partial u}{\partial t}\,dx - \frac{\partial u}{\partial t}(b+Vt,t) \cdot \frac{\partial u}{\partial x}(b+Vt,t).$$

And finally we obtain

$$\frac{d}{dt}\mathcal{E}_V(t) = \left\{ -V \left[\frac{1}{2c^2(b+Vt)} \left(\frac{\partial u}{\partial t} \right)^2 + \frac{1}{2} \left(\frac{\partial u}{\partial x} \right)^2 \right] - \frac{\partial u}{\partial t} \cdot \frac{\partial u}{\partial x} \right\} (b+Vt,t).$$

The right-hand side is a quadratic form in the two variables $\partial u/\partial t$ and $\partial u/\partial x$, whose discriminant is $1-(V/c(b+Vt))^2$. Thus, for any V such that $V \geq c^*$, we have

$$\frac{d}{dt}\mathcal{E}_V(t) \leq 0,$$

which can be rewritten as

$$\int_{b+Vt}^{+\infty} e(x,t)\,dx \leq \int_{b}^{+\infty} e(x,0)\,dx.$$

The quantity on the right vanishes, thus the quantity on the left vanishes as well. The same proof can be done on $(-\infty,a)$, which concludes the proof of the theorem. □

3.2.3 Transparent boundary condition

Here the decomposition of the solution in a part propagating to the right and a part propagating to the left becomes much more intricate. One has to introduce the theory of pseudo-differential operators, which is a very powerful but heavy tool. Instead, we shall use a PDE approach to the transparent boundary condition. We assume the data to be compactly supported in $\mathbb{R}_-$. Then the problem

$$\begin{cases} \dfrac{1}{c^2(x)} \dfrac{\partial^2 u}{\partial t^2} - \dfrac{\partial^2 u}{\partial x^2} = f \quad \text{in} \quad \mathbb{R} \times (0,T), \\ u(\cdot,0) = u^{(0)} \quad , \dfrac{\partial u}{\partial t}(\cdot,0) = u^{(1)} \quad \text{in} \quad \mathbb{R}, \end{cases}$$

is equivalent to

$$\begin{cases} \dfrac{1}{c^2(x)} \dfrac{\partial^2 u}{\partial t^2} - \dfrac{\partial^2 u}{\partial x^2} = f \quad \text{in} \quad \mathbb{R}_- \times (0,T), \\ u(.,0) = u^{(0)}, \quad \dfrac{\partial u}{\partial t}(\cdot,0) = u^{(1)} \quad \text{in} \quad \mathbb{R}_-, \\ \dfrac{\partial u}{\partial x}(0,t) - K_+(0) \dfrac{\partial u}{\partial t}(0,t) = 0 \quad \text{in} \quad (0,T), \end{cases}$$

where the transparent operator at point 0, $K_+(0)$, is defined using the exterior problem

$$\begin{cases} \dfrac{1}{c^2(x)} \dfrac{\partial^2 w}{\partial t^2} - \dfrac{\partial^2 w}{\partial x^2} = 0 \quad \text{in} \quad \mathbb{R}_+ \times (0,T), \\ w(\cdot,0) = 0, \quad \dfrac{\partial w}{\partial t}(\cdot,0) = 0 \quad \text{in} \quad \mathbb{R}_+, \\ \dfrac{\partial w}{\partial t}(0,\cdot) = g \quad \text{in} \quad (0,T). \end{cases} \tag{3.18}$$

Then the operator $K_+(0)$ is defined in a unique fashion by

$$K_+(0)g \equiv \frac{\partial w}{\partial x}(0,\cdot) \quad \text{in} \quad (0,T). \tag{3.19}$$

For general velocities, this operator cannot be written explicitly. However, when used in the context of absorbing boundary conditions, the velocity is constant in $\mathbb{R}_+$, equal to c^+, and the operator reduces to the local operator $(-1/c^+)(\partial/\partial t)$. In this case we get the transparent boundary as

$$\frac{\partial u}{\partial x}(0,t) + \frac{1}{c^+}\frac{\partial u}{\partial t}(0,t) = 0.$$

3.2.4 Domain decomposition

We cut the spatial domain $\mathbb{R}$ into I numerical domains $\Omega_i = (a_i, a_{i+1})$, $1 \le i \le I$, $a_j < a_i$ for $j < i$ and $a_1 = -\infty$, $a_{I+1} = \infty$ as described in Fig. 20.

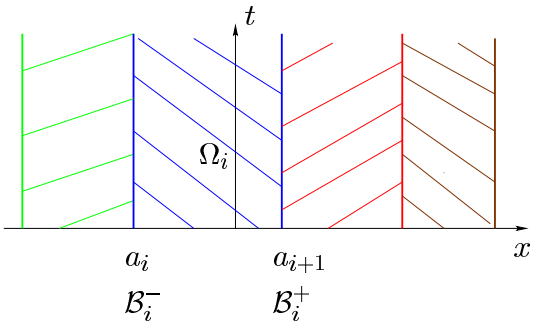

Figure 20: Decomposition into numerical domains.

We introduce the Schwarz algorithm with general transmission conditions

$$\begin{aligned}
\left(\frac{1}{c^2(x)}\partial_{tt} - \partial_{xx}\right)(u_i^{n+1}) &= f(x,t), \quad x \in \Omega_i,\ t \in (0,T),\\
\mathcal{B}_i^-(u_i^{n+1}) &= \mathcal{B}_i^-(u_{i-1}^n), \quad x = a_i,\ t \in (0,T),\\
\mathcal{B}_i^+(u_i^{n+1}) &= \mathcal{B}_i^+(u_{i+1}^n), \quad x = a_{i+1},\ t \in (0,T).
\end{aligned} \tag{3.20}$$

The optimal choice for $\mathcal{B}_i^{\pm}$ is the *transparent boundary operators*:

3.9 Theorem *The algorithm converges in I iterations on $(0,T)$ if the operators are given by*

$$\begin{aligned}
\mathcal{B}_i^- &:= (\partial_x - K_+(a_i)\partial_t),\\
\mathcal{B}_i^+ &:= (\partial_x - K_-(a_{i+1})\partial_t).
\end{aligned}$$

where the $K_\pm(a_i)$ are the transparent operators defined in (3.18) *and* (3.19).

In the case of a physical medium consisting of two media with constant velocities as in Fig. 21, $\mathcal{O}_1 = \mathbb{R}_-$ with velocity c_1, $\mathcal{O}_2 = \mathbb{R}_+$ with velocity c_2, the operators can be written

explicitly. For example,

$$K_+(x_0)g(t) = \begin{cases} \dfrac{1}{c_1} g(t), & x_0 \in \mathcal{O}_1 \\ \dfrac{1}{c_2}\left(g(t) + 2\displaystyle\sum_{k=1}^{\lfloor \frac{c_2 t}{2x_0} \rfloor} r^k g(t - 2kx_0/c_2)\right), & x_0 \in \mathcal{O}_2. \end{cases}$$

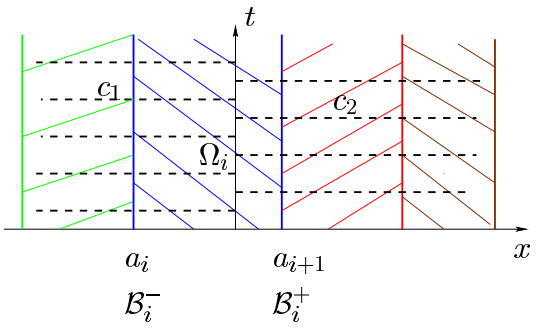

Figure 21: Physical and numerical domains.

We show now an example of convergence in three iterations for three numerical subdomains. The data are given in Table 3.

Initial data $u(x,0) = 0$, $\dfrac{\partial u}{\partial t}(x,0) = -20(4-x)e^{-10(4-x)^2}$.
Physical domains: $\mathcal{O}_1 = \mathbb{R}_-$ with velocity $c_1 = 2$, $\mathcal{O}_2 = \mathbb{R}_+$ with velocity $c_2 = 1$.
Numerical domains: $\Omega_1 = (-\infty, 1)$, $\Omega_2 = (1,3)$, $\Omega_3 = (3,+\infty)$.
Time domain $(0,8)$.

Table 3: An example with global transmission conditions.

Fig. 22 shows the convergence history.

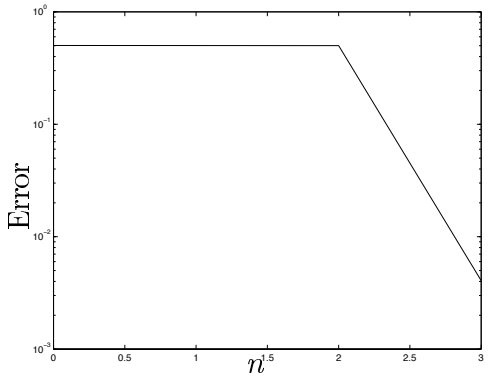

Figure 22: Error history for the optimal global transmission conditions.

Fig. 23 describes the iterates in the algorithm.

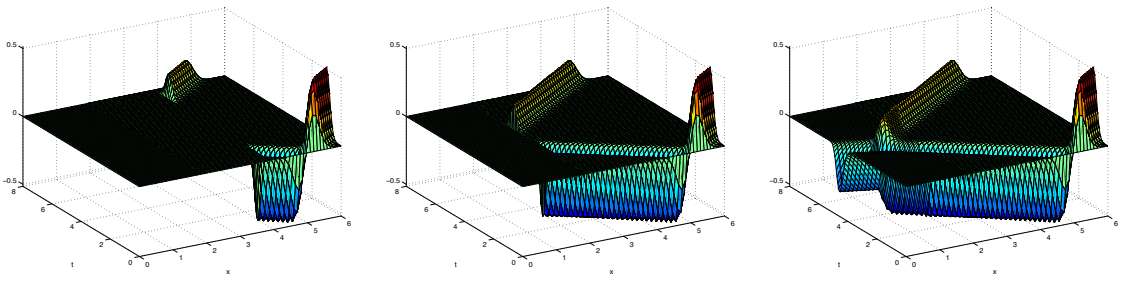

first iteration second iteration third iteration

Figure 23: Convergence in three iterations for the example in Table 3.

One can actually prove that for sufficiently small time, the optimal transmission is preserved with local operators:

3.10 Theorem *If the discontinuities lie strictly inside the domains, the algorithm converges in I iterations for*

$$T < \min_{1<i\leq I} \frac{2|a_i|}{c(a_i)}$$

with local transmission conditions

$$\mathcal{B}_i^- := \partial_x - \frac{1}{c(a_i)}\partial_t, \qquad \mathcal{B}_i^+ := \partial_x + \frac{1}{c(a_{i+1})}\partial_t. \tag{3.21}$$

In Fig. 24, we show the same example as before, except that T is chosen equal to 2. One can see that the convergence is actually achieved in two iterations.

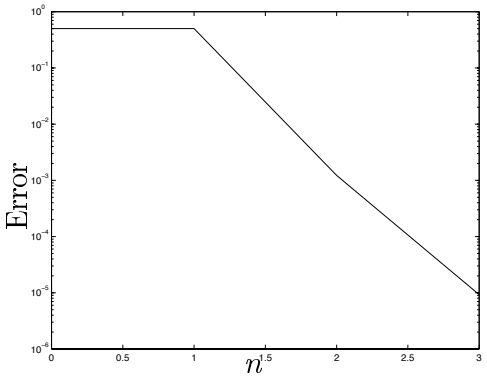

Figure 24: Error history for the local transmission conditions (3.21).

3.11 Theorem *If the velocities are constant in the numerical domains, the convergence is achieved in two iterations for*

$$T < \min_{1<i<I} \frac{|a_{i+1} - a_i|}{c((a_{i+1} + a_i)/2)}$$

with the transmission operators given by

$$\mathcal{B}_i^- := (\partial_x - \frac{1}{c^-(a_i)}\partial_t), \qquad \mathcal{B}_i^+ := (\partial_x + \frac{1}{c^+(a_{i+1})}\partial_t).$$

The proofs of Theorems 3.10 and 3.11 use the finite speed of propagation and can be found in [17].

The next example in Table 4 illustrates Theorem 3.11.

Physical domain $(0, 6)$.
Physical subdomains with velocity $c_i \in \{1, 2/3, 1/2, 3/4, 4/5\}$.
Numerical domains aligned with discontinuities.
Time domain $(0, 1)$.

Table 4: An example with six layers and a non-uniform grid.

Since we use a finite volumes scheme, there is a CFL condition (2.11). It varies with the velocity in each subdomain. The space step is the same everywhere, $\Delta x_i = 1/50$, the time step is chosen so that in each subdomain the CFL is close to 1.

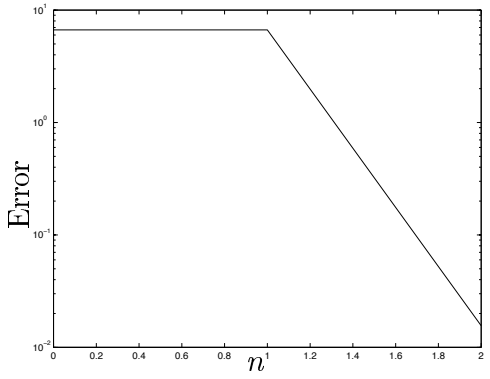

Figure 25: Convergence in two iterations with local transmission conditions on $[0, 1]$.

If we summarize the last two examples, we see convergence in two iterations with local transmission conditions on $[0, 1]$, and convergence in six iterations with local transmission conditions on $[0, 6]$. This suggests as a conclusion to use local transmission operators as in Theorem 3.11 with subdomain boundaries aligned with physical discontinuities and time windows of length

$$\min_{1<i<I} \frac{|a_{i+1} - a_i|}{c((a_{i+1} + a_i)/2)}.$$

Variable wave speed and local transmission conditions

In the case of variable wave speed there is still convergence in I iterations with the transparent transmission condition defined from the transparent operator (3.19), but this operator is non-local. With local transmission conditions (3.21), we still have a convergence result:

3.12 Theorem *Suppose the velocity is continuous at the interfaces a_i. Then on any time interval $[0,T]$, algorithm (3.20) with local transmission conditions (3.21) is well posed and converges in the energy norm,*

$$\sum_{i=1}^{I} E_{[a_i,a_{i+1}]}(u_i^k) \to 0 \quad as \quad k \to \infty. \tag{3.22}$$

Proof We introduce the forward and backward transport operators

$$\mathcal{T}_\alpha^+ = \frac{1}{\alpha}\frac{\partial}{\partial t} + \frac{\partial}{\partial x}, \qquad \mathcal{T}_\alpha^- = \frac{1}{\alpha}\frac{\partial}{\partial t} - \frac{\partial}{\partial x},$$

where α is a positive real number. The standard energy estimate becomes in this case for positive α and β

$$\frac{d}{dt}[E_{[a,b]}(u)(t)] + \frac{\alpha}{4}[\mathcal{T}_\alpha^+ u(a,t)]^2 + \frac{\beta}{4}[\mathcal{T}_\beta^- u(b,t)]^2 = \frac{\alpha}{4}[\mathcal{T}_\alpha^- u(a,t)]^2 + \frac{\beta}{4}[\mathcal{T}_\beta^+ u(b,t)]^2.$$

By writing the energy identity in every subdomain, using the transmission conditions and adding the corresponding equations in i and n we obtain (3.22). □

We now give an example. The velocity profile, which is a typical underwater profile, was obtained from [27] and it is given as a function of depth by

$$c(x) = \begin{cases} 300 \text{ m/s} & x < 0 \quad \text{(above ground)} \\ 1500 - x/12 \text{ m/s} & 0 < x < 120 \\ 1320 + x/12 \text{ m/s} & 120 < x < 240 \\ 1505 \text{ m/s} & x > 240. \end{cases} \tag{3.23}$$

The numerical domains are $\Omega_1 = [0,300]$ and $\Omega_2 = [300,600]$. We start with the errors in Table 5. Fig. 26 shows the first ans second iteration.

Iteration	0	1	2	3
$\|\|u - u_k\|\|_\infty$	5e + 00	5e + 00	9.9e − 03	6.2e − 04

Table 5: Convergence behavior of the algorithm for the variable sound speed profile (3.23).

The algorithm converges again to the accuracy of the scheme in two iterations, even though the sound speed is variable in this example. This is because the variation is small in scale and thus the local approximations to the transmission conditions are sufficiently accurate to lead to the convergence in two steps. Note also that, continuing the iteration, the error is further reduced.

3.3 The discrete domain decomposition algorithm

We first decribe the scheme, and then give a convergence result.

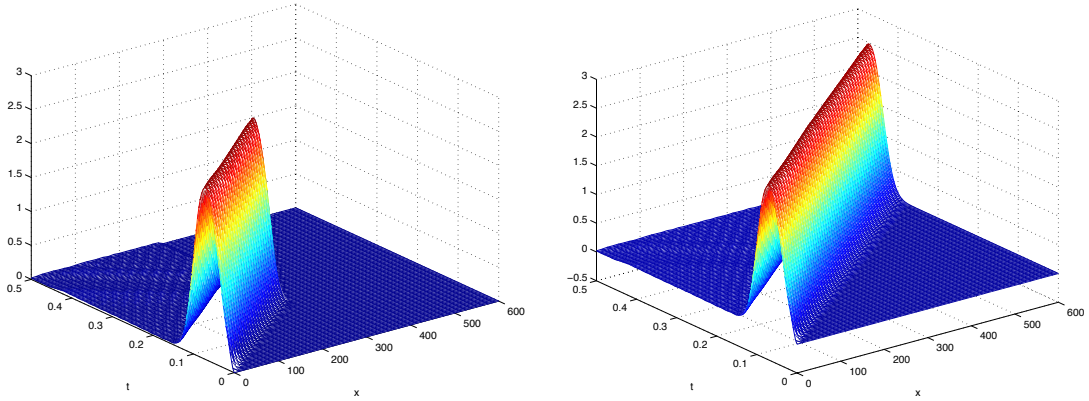

first iteration second iteration

Figure 26: Convergence in two iterations for the underwater example (3.23).

3.3.1 Description of the scheme

In order to take the transmission conditions into account, we use a vertex-centered finite volume method [14], as described in Fig. 27. We discretize the wave equation (3.17) on each subdomain $\Omega_i \times (0,T)$, $i = 1,\dots,I$, separately, using a finite volume discretization on rectangular grids. For simplicity of the exposition we set $f = 0$. We allow non-matching grids on different subdomains, with $J_i + 2$ points in space numbered from 0 up to $J_i + 1$ and $\Delta x_i = (a_{i+1} - a_i)/(J_i + 1)$, and $N_i + 1$ grid points in time with $\Delta t_i = T/N_i$, numbered from 0 up to N_i. Note that for the exposition here we choose uniform spacing in time per subdomain, but the techniques developed are not limited to this special case. We denote the numerical approximation to $u_i^k(a_i + j\Delta x_i, n\Delta t_i)$ on Ω_i at iteration step k by $U_i^k(j,n)$.

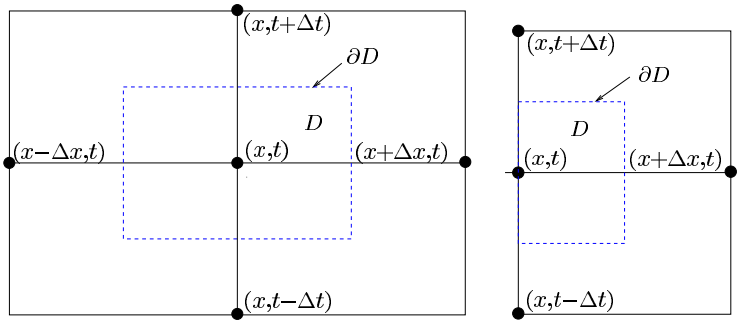

interior point boundary point

Figure 27: Control volumes for the scheme.

In the interior of the domains, this leads to the leapfrog scheme

$$\left(\frac{1}{C_i^2(j)} D_t^+ D_t^- - D_x^+ D_x^-\right)(U_i^{k+1})(j,n) = 0 \quad 1 \le j \le J_i,\ 1 \le n \le N_i,$$

with the usual notations

$$D_t^+(U)(j,n) = \frac{U(j,n+1)-U(j,n)}{\Delta t},$$
$$D_t^-(U)(j,n) = \frac{U(j,n)-U(j,n-1)}{\Delta t},$$
$$D_t^0 = \frac{D_t^+ + D_t^-}{2},$$

and the same for the variable x. $C_i(j)$ is a discrete function approximating $c(a_i + j\Delta x_i)$. The discrete transmission conditions are obtained by integrating the equation on the half-cell, and using the continuous transmission condition.

We first glue together the grids on two neighbouring domains. Let $I_n =]t_n, t_{n+1}[$ be a sequence of intervals such that $\bigcup_{n=0}^{N} \bar{I}_n = [0,T]$. The space $\mathbb{R}^{N+1}$ is equipped with the scalar product

$$(\boldsymbol{v},\boldsymbol{w})_{N+1} = \sum_{n=0}^{N} |I_n| v_n w_n,$$

where $|I_n|$ is the length of the interval I_n. We define the map $\mathbb{F}$ from $\mathbb{R}^{N+1}$ to $L^2(0,T)$ which maps $\boldsymbol{v}$ to the function f equal to v_n in I_n for $0 \le n \le N$, and the operator $\mathbb{E}$ from $L^2(0,T)$ to $\mathbb{R}^{N+1}$ which maps f to the sequence $v_n = 1/|I_n| \int_{I_n} f(t)\,dt$.

We denote by $\mathbb{F}_i$ and $\mathbb{E}_i$ the operators corresponding to the grid in Ω_i, and we define the operator $\mathbb{P}_{i,j} : \mathbb{R}^{N_i+1} \to \mathbb{R}^{N_j+1}$ as

$$\mathbb{P}_{i,j} := \mathbb{E}_j \circ \mathbb{F}_i. \tag{3.24}$$

The discrete algorithm is now defined by

$$\begin{gathered}
\left(\frac{1}{C_i^2(j)} D_t^+ D_t^- - D_x^+ D_x^-\right)(U_i^{k+1})(j,n) = 0 \quad 1 \le j \le J_i,\ 1 \le n \le N_i, \\
\left(\frac{\Delta x}{C_i^2(j)} D_t^+ - \frac{\Delta t \Delta x}{2} D_x^+ D_x^-\right)(U_i^{k+1})(j,0) \frac{\Delta x}{C_i^2(j)} U_t(j) = 0 \quad 1 \le j \le J_i, \\
B_i^-(U_i^{k+1})(0,\cdot) = \mathbb{P}_{i-1,i} \widetilde{B}_i^-(U_{i-1}^k)(J_{i-1}+1,\cdot), \\
B_i^+(U_i^{k+1})(J_i+1,\cdot) = \mathbb{P}_{i+1,i} \widetilde{B}_i^+(U_{i+1}^k)(0,\cdot),
\end{gathered} \tag{3.25}$$

where the operators $\mathbb{P}_{i\pm1,i}$ are defined in (3.24), the discrete transmission operators $B_i^{\pm}$ are for $n \ge 1$ given by

$$\begin{aligned}
B_i^+(U_i)(J_i+1,n) &= \left(\frac{\Delta x_i}{2C_i^2(J_i+1)} D_t^+ D_t^- + D_x^- + \frac{1}{C_{i+1}(0)} D_t^0\right)(U_i)(J_i+1,n), \\
B_i^-(U_i)(0,n) &= \left(\frac{\Delta x_i}{2C_i^2(0)} D_t^+ D_t^- - D_x^+ + \frac{1}{C_{i-1}(J_{i-1}+1)} D_t^0\right)(U_i)(0,n),
\end{aligned} \tag{3.26}$$

and the extraction operators $\widetilde{B}_i^{\pm}$ are for $n \ge 1$

$$\begin{aligned}
\widetilde{B}_i^+(U_{i+1})(0,n) &= \left(-\frac{\Delta x_{i+1}}{2C_{i+1}^2(0)} D_t^+ D_t^- + D_x^+ + \frac{1}{C_{i+1}(0)} D_t^0\right)(U_{i+1})(0,n), \\
\widetilde{B}_i^-(U_{i-1})(J_{i-1}+1,n) &= \\
&\left(-\frac{\Delta x_{i-1}}{2C_{i-1}^2(J_{i-1}+1)} D_t^+ D_t^- - D_x^- + \frac{1}{C_{i-1}(J_{i-1}+1)} D_t^0\right)(U_{i-1})(J_{i-1}+1,n).
\end{aligned} \tag{3.27}$$

The transmission conditions for $n = 0$ are obtained by replacing D_t^0 by D_t^+ and $D_t^+ D_t^-/2$ by $D_t^+/\Delta t$, and introducing the initial velocity. Note that in contrast to the continuous case, the transmission and extraction operators are different. In addition, for non-matching grids, we introduced projection operators which are non-linear. The four operators involved in (3.26), (3.27) are Lax-Wendroff type approximations of the continuous operators (they correspond to the discrete absorbing boundary conditions described in [19]).

3.3.2 Stability and convergence

All the proofs here are very long and intricate, so we refer to [17] for details. For continuous velocities on the interfaces, we have a first convergence result using discrete energy estimates.

3.13 Theorem *Assume that the velocity is continuous on the interfaces a_i. If the CFL condition is satisfied by the discretization in each subdomain, then the non-overlapping discrete Schwarz algorithm with projections* (3.25) *converges on any time interval* $[0,T]$ *in the energy norm:*

$$\sum_{i=1}^{I} E_{N_i}(U_i^k) \to 0 \quad as \quad k \to +\infty.$$

Let us recall that in the case of piecewise continuous velocities we recommended that the numerical domain be aligned with the physical discontinuities. In the case of two velocities, when the time step is constant, we have a partial result using the discrete Laplace transform, or z transform (see [35]),

$$U_i^k(j,n) = a_i^k z^n r_i^j, \qquad z = e^{(\eta + i\omega)\Delta t}.$$

3.14 Theorem *If $(c_1 - c_2)(\gamma_1 - \gamma_2) \geq 0$, there exists a positive real constant $C > 0$ such that for $\eta \Delta t \ll 1$, we have*

$$||U_i^k(j,n)||_{\Omega_i,\eta,\Delta t} \leq (1 - C\eta\Delta t)^{\lfloor p/2 \rfloor} \max_l (||U_l^0(j,n)||_{\Omega_l,\eta,\Delta t}), \quad i = 1,2.$$

In particular, there is an interface wave: if $z = e^{i\omega\Delta t}$, for $\sin^2(\omega\Delta t/2) > \gamma_i$, there is a solution

$$U_i^{2k}(0,n) = De^{i\omega\Delta t(n+Vk)},$$

where V depends on γ_1, γ_2, and c_1/c_2.

4 Paraxial operators and applications in two dimensions

We mainly concentrate here on the techniques stemming from the theory of pseudodifferential operators [12, 13, 4], but we shall also call on other theories leading to useful absorbing boundary conditions.

4.1 The paraxial problem

The goal is to approximate the equation by a simpler one whose solution propagates in a particular direction. There are many applications, like for instance electromagnetic waves in atmospherical layers, acoustic waves in the ocean, techniques of migration in oil recovery, and the computation of guided waves in optical fibers. We start with the homogeneous wave equation in two dimensions

$$\frac{1}{c^2}\frac{\partial^2 u}{\partial t^2} - \frac{\partial^2 u}{\partial x_1^2} - \frac{\partial^2 u}{\partial x_2^2} = 0.$$

We look at the functions of the form

$$u = e^{i(\boldsymbol{k}\cdot\boldsymbol{x}-\omega t)} \tag{4.1}$$

which is a plane wave solution if and only if the frequency ω and the wave vector $\boldsymbol{k} = (k_1, k_2)$ are linked through the dispersion relation

$$\frac{\omega^2}{c^2} = |\boldsymbol{k}|^2 = k_1^2 + k_2^2.$$

If we introduce the angle θ defined by

$$\sin\theta = c\frac{k_1}{\omega}, \qquad \cos\theta = c\frac{k_2}{\omega},$$

we get the *slowness curve* depicted in Fig. 28.

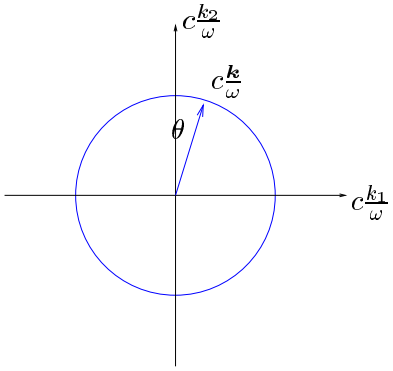

Figure 28: Slowness curve for the wave equation.

4.1.1 The paraxial approximation

Suppose we want to approximate as well as possible the waves propagating upwards, i.e. in the $x_2 > 0$ direction (in geophysics it is usually the depth direction). The dispersion relation of the waves propagating upwards is

$$c\frac{k_2}{\omega} = \sqrt{1 - \left(c\frac{k_1}{\omega}\right)^2}, \tag{4.2}$$

which corresponds to the upper half of the slowness plane. We want to approximate the square root in (4.2) by a function of ck_1/ω which can be, modulo a denominator, the dispersion relation of a partial differential operator. The only way is to use rational fractions [28]

$$(1-X)^{1/2} \approx r(X) = \frac{p_m(X)}{q_n(X)},$$

where p_m and q_n are polynomials in x of degree m and n, respectively. The classical approximations [8, 13, 4] are the Taylor or Padé expansion of low order for small θ.

$$\begin{aligned} \textit{Taylor of order } 0: &\quad c\frac{k_2}{\omega} \approx 1, \\ \textit{Taylor of order } 1: &\quad c\frac{k_2}{\omega} \approx 1 - \frac{1}{2}\left(c\frac{k_1}{\omega}\right)^2, \\ \textit{Padé of order } 1: &\quad c\frac{k_2}{\omega} \approx \frac{1-3/4(ck_1/\omega)^2}{1-1/4(ck_1/\omega)^2}. \end{aligned}$$

To recover the partial differential equations, we clear the denominators, and get the following table, where on the right we put the usual name of these equations.

$$\frac{1}{c}\frac{\partial u}{\partial t} + \frac{\partial u}{\partial x_2} = 0, \quad \textit{transport equation}, \tag{4.3}$$

$$\frac{1}{c}\frac{\partial^2 u}{\partial t^2} + \frac{\partial^2 u}{\partial x_2 \partial t} - \frac{c}{2}\frac{\partial^2 u}{\partial x_1^2} = 0, \quad \textit{parabolic or } 15^\circ \textit{ equation}, \tag{4.4}$$

$$\frac{1}{c}\frac{\partial^3 u}{\partial t^3} + \frac{\partial^3 u}{\partial x_2 \partial t^2} - \frac{3c}{4}\frac{\partial^3 u}{\partial x_1^2 \partial t} - \frac{c^2}{4}\frac{\partial^3 u}{\partial x_1^2 \partial x_2} = 0, \quad 45^\circ \textit{ equation}. \tag{4.5}$$

These equations were called 15° (resp. 45°) because the geophysicists considered them to be accurate for propagation angles up to 15° (resp. 45°) [8]. This strategy can be generalized to higher degrees [13, 4, 28, 20] by introducing the approximate equation

$$c\frac{k_2}{\omega} = r((ck_1/\omega)^2) = \frac{p_m((ck_1/\omega)^2)}{q_n((ck_1/\omega)^2)} = R(ik_1, i\omega). \tag{4.6}$$

Let $d = \max(2m, 2n+1)$ be the total order. By clearing the denominators we obtain a *dispersion relation*

$$\omega^{d-1} k_2 q_n((ck_1/\omega)^2) - \omega^d p_m((ck_1/\omega)^2) = 0,$$

which is of the general form $\mathcal{L}(-i\omega, ik_1, ik_2) = 0$ with $d^\circ\mathcal{L} = d$. It is the dispersion relation of

$$\mathcal{L}(\partial_t, \partial_{x_1}, \partial_{x_2})u = 0. \tag{4.7}$$

Note that the operator $\mathcal{L}$ is of first order in the x_2-direction. The absorbing boundary conditions obtained by Taylor approximations of order three or more lead to ill-posed problems [13]. Various strategies can be applied to approximate the symbol (4.2) depending on the applications, for instance:

- *Padé*: $\sqrt{1-y^2} - r(y^2) = O(y^{2m+2n+1})$ [13],
- *Tchebyshev*: minimize $\|\sqrt{1-y^2} - r(y^2)\|_\infty$ [20],
- *Least squares*: minimize $\|\sqrt{1-y^2} - r(y^2)\|_2$ [28],
- *Interpolation* at arbitrary points [20, 22].

4.1.2 The paraxial problem

The physical problem we start with is the wave equation in two dimensions with given initial conditions

$$\begin{cases} \dfrac{1}{c^2}\dfrac{\partial^2 u}{\partial t^2} - \dfrac{\partial^2 u}{\partial x_1^2} - \dfrac{\partial^2 u}{\partial x_2^2} = 0 \quad \text{in} \quad \mathbb{R}^2 \times (0,T), \\ u(0,.) = u^{(0)}, \quad \dfrac{\partial u}{\partial t}(0,.) = u^{(1)} \quad \text{in} \quad \mathbb{R}^2. \end{cases} \tag{4.8}$$

The paraxial operator (4.7) related to the paraxial approximation is of order d in time. If d is greater than 3 we need more initial values. They can be obtained by differentiating the wave equation. This can be expressed by

$$\mathcal{P}_C \begin{cases} \mathcal{L}u = 0 \quad \text{in} \quad \mathbb{R}^2 \times (0,T) \\ \dfrac{\partial^p u}{\partial t^p} u(0,.) = u^{(p)} \quad \text{in} \quad \mathbb{R}^2, \ 0 \le p \le d-1. \end{cases} \tag{4.9}$$

In fact, these operators are never used as high degree operators, but rather as a system of second degree operators, as we will see in Section 4.3.1.

4.2 Absorbing boundary conditions

As we saw in Section 3, the goal here is to truncate the computational domain : suppose we want to compute the solution of the wave equation only in a part Ω_{ref} of $\mathbb{R}^2$. We introduce a computational domain Ω_{comp} and boundary conditions on the boundary $\partial\Omega_{\text{comp}}$ of Ω_{comp} such that the waves can leave the computational domain with as low reflection as possible, which in turn implies that we can place the computational domain close to the reference domain Ω_{ref}. The applications are countless in engineering like geophysics, aeronautics, radars, etc.

4.2.1 Absorbing boundary conditions for a half-plane

We consider waves propagating in the half-plane $x_2 < 0$. The waves propagating upwards are given by (4.2), of the form $e^{i(\boldsymbol{k}\cdot\boldsymbol{x}-\omega t)}$, with $ck_2/\omega = +\sqrt{1-(ck_1/\omega)^2}$. Suppose a general boundary condition is given at $x_2 = 0$. We isolate the derivative in the x_2-direction,

$$\mathcal{M}(\partial_t, \partial_{x_1}, \partial_{x_2})u \equiv \frac{\partial u}{\partial x_2} + \mathcal{B}(\partial_t, \partial_{x_1})u = 0.$$

Let a wave U^{Inc} be impinging on the boundary. By the Snell or Descartes law shown in Fig. 29, the reflected wave is $U^{\text{Ref}} = Re^{i(-k_1x_1+k_2x_2-\omega t)}$, such that

$$\mathcal{M}(U^{\text{Inc}} + U^{\text{Ref}}) = 0,$$

which can be rewritten as

$$ik_2 + \mathcal{B}(-i\omega, ik_1) + R(-ik_2 + \mathcal{B}(-i\omega, ik_1)) = 0.$$

Thus the boundary condition $\mathcal{M}u = 0$ is a transparent boundary condition if its symbol is given by

$$\mathcal{B}(-i\omega, ik_1) \equiv -i\frac{\omega}{c}\sqrt{1-\left(c\frac{k_1}{\omega}\right)^2},$$

and the *transparent boundary operator is the exact paraxial operator*. As absorbing boundary condition we will impose the approximations $\mathcal{L}$ derived in Section 4.1.1.

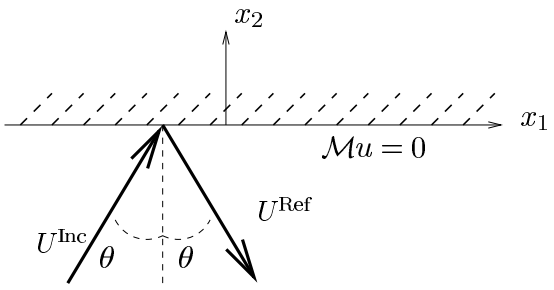

Figure 29: Reflection on the boundary $x_2 = 0$.

4.2.2 The initial boundary value problem

We suppose that the initial data are compactly supported in the half-plane $\mathbb{R}^2_- = \mathbb{R}_- \times \mathbb{R}$, and we replace the Cauchy problem (4.8) by the initial boundary value problem

$$\mathcal{P}_L \begin{cases} \dfrac{1}{c^2}\dfrac{\partial^2 u}{\partial t^2} - \dfrac{\partial^2 u}{\partial x_1^2} - \dfrac{\partial^2 u}{\partial x_2^2} = 0 \quad \text{in} \quad \mathbb{R}^2_- \times (0,T), \\ u(0,.) = u^{(0)}, \quad \dfrac{\partial u}{\partial t}(0,.) = u^{(1)} \quad \text{in} \quad \mathbb{R}^2_-, \\ \mathcal{L}u(t,0) = 0 \quad \text{in} \quad (0,T), \end{cases} \tag{4.10}$$

where $\mathcal{L}$ is any of the paraxial approximations defined in Section 4.1.1, as for instance in (4.3), (4.4) or (4.5). The quality of the approximation is measured by the reflection coefficient. It has been shown that for the absorbing boundary conditions cited above the reflection coefficient is equal to

$$R = \left(\frac{\cos\theta - 1}{\cos\theta + 1}\right)^n.$$

This is a general result for Padé approximation of type (n, n) [13].

Fig. 30 shows the historical example given by R. W. Clayton and B. Engquist in 1977 [9]. The initial value is a spherical compressional wave. On the first line the second order absorbing boundary condition (4.4) is imposed , and on the second line the perfectly reflecting Dirichlet boundary condition is imposed.

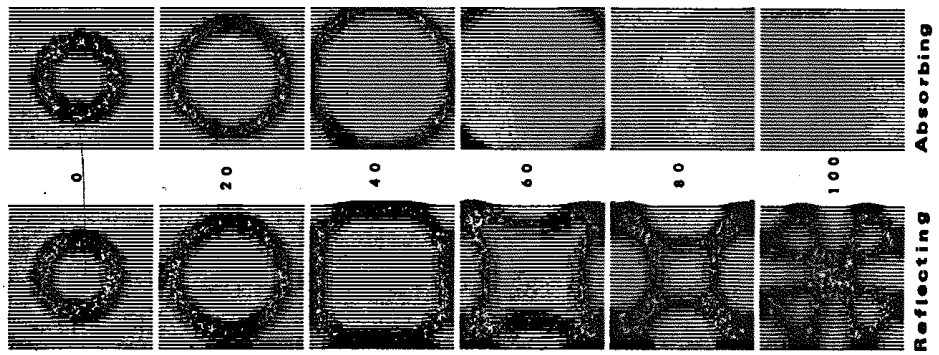

Figure 30: A historical example from [9].

4.3 Well-posedness results

We consider the paraxial problem $\mathcal{P}_C$ defined in (4.9) and the half-plane problem $\mathcal{P}_L$ defined in (4.10). $\mathcal{L}$ is the operator $\mathcal{L}(\partial t, \partial x_1, \partial x_2)$. Its symbol is $l(\omega, \boldsymbol{k}) = \mathcal{L}(i\omega, i\boldsymbol{k})$.

4.1 Remark This is the sign choice made by the analysts. It differs from the convention chosen by the physicists in (4.1).

We first give a classical result on well-posedness for Cauchy problems (for all these basic results see for instance [26]):

$$\begin{gathered} \mathcal{P}_C \textit{ well-posed} \\ \Updownarrow \\ \mathcal{L} \textit{ hyperbolic} \\ \Updownarrow \\ \forall \boldsymbol{k} \in \mathbb{R}^2, \quad l(\omega, \boldsymbol{k}) = 0 \Longrightarrow \omega \in \mathbb{R} \end{gathered}$$

There is also a characterisation of well-posed initial boundary value problems:

$$\begin{gathered} \mathcal{P}_L \textit{ well-posed} \\ \Updownarrow \\ \forall k_1 \in \mathbb{R},\ \forall k_2 \in \mathbb{C},\ \Im k_2 \geq 0, \\ \left.\begin{aligned} l(\omega, \boldsymbol{k}) &= 0 \\ \omega^2 = k_1^2 + k_2^2, \quad \Re\omega &\leq 0 \end{aligned}\right\} \implies (\omega, \boldsymbol{k}) = (0, \boldsymbol{0}) \end{gathered}$$

The following results have been proved in [20]:

4.2 Theorem *Problem $\mathcal{P}_C$ is well-posed if and only if the rational fraction $r(X)$ in (4.6) can be expanded as*

$$r(X) = a - \beta X - \sum_{k=1}^{n} \frac{\beta_k X}{1 - \gamma_k^2 X}, \tag{4.11}$$

where the coefficients a, β_k are such that $a > 0$, $\beta \geq 0$, $\beta_k > 0$ for $1 \leq k \leq n$.

4.3 Theorem *Problem $\mathcal{P}_L$ is well-posed if and only if we have property (4.11), and furthermore for all X in $[-1, 1]$, the value of the function $r(X)$ defined in (4.11) is positive.*

These results give a necessary condition for well-posedness:

4.4 Corollary *If problems $\mathcal{P}_L$ and $\mathcal{P}_C$ are well-posed, then $n \leq m \leq n + 1$.*

The well-posedness for the two problems are related by the following result:

4.5 Corollary *If problem $\mathcal{P}_L$ is well-posed, then problem $\mathcal{P}_C$ is well-posed.*

In the same paper the following useful criterium is also derived:

$$\begin{gathered} \mathcal{P}_L \textit{ well-posed} \\ \Updownarrow \\ \left\{\begin{array}{l} n \leq m \leq n+1 \quad \textit{and} \\ r(y) - \sqrt{1-y^2} \textit{ has } 2(m+n+1) \textit{ roots in } \mathbb{C} -]-\infty, -1] - [1, +\infty[. \end{array}\right. \end{gathered}$$

4.3.1 Writing the operator as a system

As mentioned before, the expression $\mathcal{L}(\partial_t, \partial_{x_1}, \partial_{x_2})u = 0$ is not very easy to handle, especially when it comes to discretization. Instead, following [28], we turn back to the formula

$$\left[-c\frac{k_2}{\omega} + 1 - \sum_{k=1}^{m} \frac{\beta_k c^2 k_1^2}{\omega^2 - \gamma_k c^2 k_1^2}\right] \hat{u} = 0,$$

and we introduce auxiliary unknowns φ_k by their Fourier transforms

$$\frac{c^2 k_1^2}{\omega^2 - \gamma_k c^2 k_1^2} \hat{u} = \hat{\varphi}_k,$$
$$\left(-c\frac{k_2}{\omega} + 1\right) \hat{u} - \sum_{k=1}^{m} \beta_k \hat{\varphi}_k = 0,$$

which leads to the system of partial differential equations

$$\begin{cases} \dfrac{\partial u}{\partial t} + c\dfrac{\partial u}{\partial x_2} - \displaystyle\sum_{k=1}^{m} \beta_k \frac{\partial \varphi_k}{\partial t} = 0, \\ \dfrac{1}{c^2}\dfrac{\partial^2 \varphi_k}{\partial t^2} - \gamma_k^2 \dfrac{\partial^2 \varphi_k}{\partial x_1^2} = \dfrac{\partial^2 u}{\partial x_1^2}, \quad 1 \le k \le m, \end{cases}$$

with initial conditions on the functions φ_k:

$$\varphi_k(0, x) = 0.$$

Notice that the new unknowns φ_k are active only in the transverse direction, which makes this formula very easy to discretize [6].

There is an alternative theory by Higdon on absorbing boundary conditions [22]. He writes any well-posed absorbing boundary condition as a product of first-order transport operators, which makes the discretization even easier. But this involves a high order operator in the x_2-direction.

4.3.2 Bayliss and Turkel operators

We describe here another approach of absorbing boundary conditions, relying on a far-field expansion of the solution of the wave equation in three dimensions [5],

$$u(r, \theta, \varphi, t) = r^{-1} e^{ik(r-ct)} \sum_{n=0}^{\infty} r^{-n} u_n(\theta, \varphi). \tag{4.12}$$

Defining the Sommerfeld operator $\mathcal{S}$ by

$$\mathcal{S} = \left(\frac{\partial}{\partial r} + \frac{1}{c}\frac{\partial}{\partial t}\right),$$

we note, using (4.12), that we have in the three-dimensional case

$$\lim_{r\to\infty} r\left(\frac{\partial u}{\partial r}+\frac{1}{c}\frac{\partial u}{\partial t}\right)=0,$$

and more generally in dimension d

$$\lim_{r\to\infty} r^{(d-1)/2}\left(\frac{\partial u}{\partial r}+\frac{1}{c}\frac{\partial u}{\partial t}\right)=0.$$

A. Bayliss and E. Turkel [5] proposed an iterative improvement of the Sommerfeld condition, in the following way. For the Sommerfeld operator we have $\mathcal{S}u = O(r^{-2})$. Introducing an "augmented" version of the Sommerfeld operator

$$\mathcal{B}_1 = \mathcal{S} + \frac{1}{r},$$

we have by (4.12)

$$\mathcal{B}_1 u = O\left(\frac{1}{r^3}\right).$$

The operator $\mathcal{B}_1$ is the first order Bayliss and Turkel operator. Following the same approach, Bayliss and Turkel define a hierarchy of operators

$$\mathcal{B}_k = \left(\mathcal{S} + \frac{2k-1}{r}\right)\mathcal{B}_{k-1}.$$

A short calculation shows that for any k we have

$$\mathcal{B}_k u = \sum_{n=1}^{\infty} a_n^k u_n r^{-(n+k)},$$

with the recursion relation

$$u_n = e^{ik(r-ct)}u_{n-1}, \qquad a_n^k = (-1)^k(n-1)\cdots(n-k).$$

Thus $\mathcal{B}_k$ absorbs the first k terms of the expansion (4.12):

$$\mathcal{B}_k u = O\left(\frac{1}{r^{2k+1}}\right).$$

4.4 Domain decomposition method

This part is work in progress, see [16], and we sketch ideas only. Let $\mathbb{R}^2$ be divided into two subdomains $\Omega_1 = \mathbb{R}\times(-\infty, L)$ and $\Omega_2 = \mathbb{R}\times(0,\infty)$ with an overlap as depicted in Fig. 31. The boundaries are $\Gamma_1 = \mathbb{R}\times\{L\}$ and $\Gamma_2 = \mathbb{R}\times\{0\}$.

The natural extension of the classical Schwarz algorithm is then

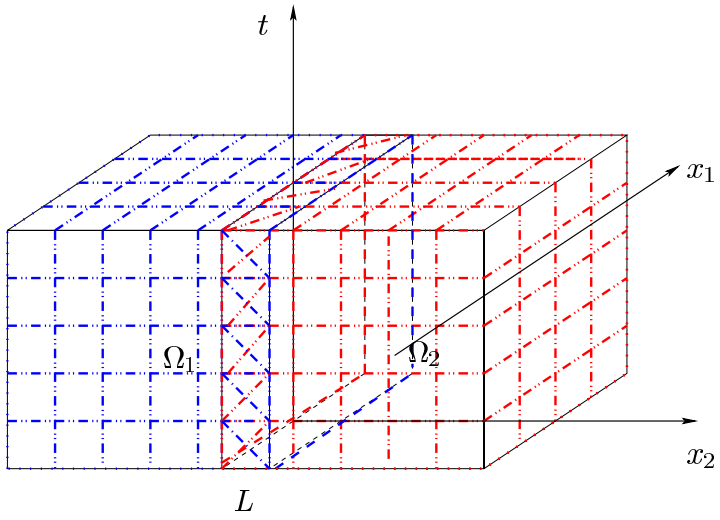

Figure 31: Domain decomposition in two half-planes.

$$\left.\begin{aligned}
&\frac{1}{c^2}\frac{\partial^2 u_i^{n+1}}{\partial t^2} - \frac{\partial^2 u_i^{n+1}}{\partial x_1^2} - \frac{\partial^2 u_i^{n+1}}{\partial x_2^2} = 0 \quad \text{in} \quad \Omega_i \times (0,T),\\
&\text{with the initial conditions}\\
&u_i^{n+1}(0,.) = u^{(0)}, \quad \frac{\partial}{\partial t} u_i^{n+1}(0,.) = u^{(1)} \quad \text{in} \quad \Omega_i,\\
&\text{and the transmission conditions}\\
&u_1^{n+1} = u_2^n \quad \text{on} \quad \Gamma_1 \times (0,T), \qquad u_2^{n+1} = u_1^n \quad \text{on} \quad \Gamma_2 \times (0,T).
\end{aligned}\right\} \tag{4.13}$$

The following result is a straightforward consequence of the finite speed of propagation:

4.6 Theorem *The Schwarz algorithm converges for a number of iterations* $n > T\overline{c}/L$ *with* $\overline{c} := \sup_{\mathbf{x}\in\Omega} c(\mathbf{x})$.

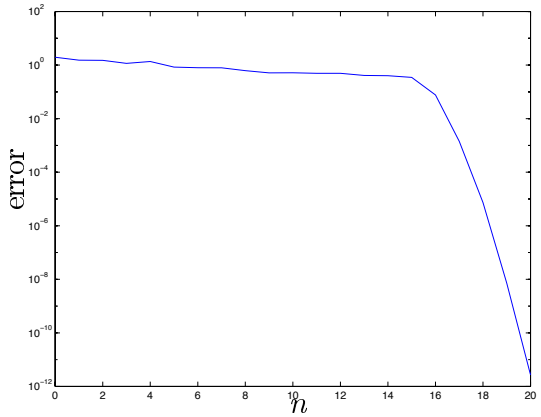

Figure 32: Convergence history for the Schwarz algorithm.

Fig. 32 shows the curve of convergence for the wave equation with speed 1 on the square $0 < x, y < 1$, for the time interval $0 < t < T = 1.2$. We have two subdomains and the overlap is $L = 0.08$. The theory predicts convergence after 15 iterations.

4.7 Remark The result in Theorem 4.6 is very general. The difficulty with many subdomains is the construction of the subdomains. In Figs. 33 and 34 we illustrate the strategy we suggest from classical Schwarz methods: first we divide the domain into squares without overlap, and then we add layers.

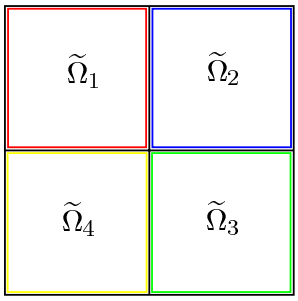

Figure 33: Non-overlapping domains.

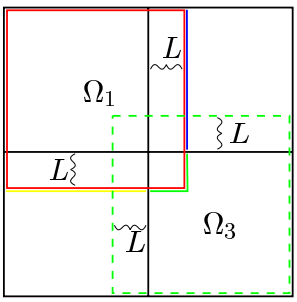

Figure 34: Overlapping domains.

4.4.1 Optimal transmission conditions

We introduce the algorithm with general transmission conditions

$$\left(\frac{\partial}{\partial x_2} + \Lambda_1(\partial_t, \partial_{x_1})\right) u_1^{n+1} = \left(\frac{\partial}{\partial x_2} + \Lambda_1(\partial_t, \partial_{x_1})\right) u_2^n, \quad x_2 = L,$$
$$\left(\frac{\partial}{\partial x_2} + \Lambda_2(\partial_t, \partial_{x_1})\right) u_2^{n+1} = \left(\frac{\partial}{\partial x_2} + \Lambda_2(\partial_t, \partial_{x_1})\right) u_1^n, \quad x_2 = 0,$$

and we use a plane wave analysis. The error (U_i^n) is given by

$$U_i^n = a_i^n e^{i(\mathbf{k^i}\cdot\mathbf{x} - \omega t)},$$

with the dispersion relations

$$c\frac{k_2^2}{\omega} = \sqrt{1 - \left(c\frac{k_1^2}{\omega}\right)^2}, \qquad k_1^2 = k_1^1, \qquad k_2^2 = -k_2^1,$$

and the relation between the coefficients over a double iteration is

$$a_1^{n+1} = \frac{ik_2^1 + \lambda_1}{-ik_2^1 + \lambda_1} \cdot \frac{-ik_2^1 + \lambda_2}{ik_2^1 + \lambda_2} e^{+2ik_2^1 L} a_1^{n-1}.$$

We define the *convergence rate* of the algorithm by

$$\rho(\mathbf{k},\omega) = \frac{-i\omega\sqrt{1-(ck_1^1/\omega)^2} + c\lambda_1}{i\omega\sqrt{1-(ck_1^1/\omega)^2} + c\lambda_1} \cdot \frac{i\omega\sqrt{1-(ck_1^1/\omega)^2} + c\lambda_2}{-i\omega\sqrt{1-(ck_1^1/\omega)^2} + c\lambda_2} e^{-2ic\omega\sqrt{1-(ck_1^1/\omega)^2}L}, \quad (4.14)$$

and the coefficients are now related by

$$a_1^{n+1} = \rho(\mathbf{k},\omega)_1^{n-1}.$$

It is evident from (4.14) that by choosing

$$\lambda_1 = \frac{i\omega}{c}\sqrt{1-\left(c\frac{k_1^1}{\omega}\right)^2} \quad \text{and} \quad \lambda_2 = -\frac{i\omega}{c}\sqrt{1-\left(c\frac{k_1^1}{\omega}\right)^2},$$

the algorithm converges in two iterations. Furthermore the result is general: for these transmission conditions, with I subdomains, the convergence is achieved in I iterations. Thus: *The optimal transmission conditions correspond to the transparent operator.*

4.4.2 Approximations of the optimal transmission conditions

We approximate the symbols λ_1 and λ_2 at normal incidence, i.e. for small values of ck_1^1/ω, by $\pm i\omega/c$, and we obtain

$$\Lambda_{12} \approx \pm\frac{1}{c}\frac{\partial}{\partial t},$$

which gives as transmission conditions

$$\begin{cases} \left(\dfrac{\partial}{\partial x_2} + \dfrac{1}{c}\dfrac{\partial}{\partial t}\right) u_1^{n+1} = \left(\dfrac{\partial}{\partial x_2} + \dfrac{1}{c}\dfrac{\partial}{\partial t}\right) u_2^n, & x_2 = L, \\ \left(\dfrac{\partial}{\partial x_2} - \dfrac{1}{c}\dfrac{\partial}{\partial t}\right) u_2^{n+1} = \left(\dfrac{\partial}{\partial x_2} - \dfrac{1}{c}\dfrac{\partial}{\partial t}\right) u_1^n, & x_2 = 0. \end{cases} \quad (4.15)$$

We show in Fig. 35 the curve of convergence for this algorithm, compared to the classical Schwarz algorithm. The data are the same as in Fig. 32.

With this kind of transmission conditions, it is also possible to work without overlap. For further developments on this issue we refer to [16].

We have already seen some links between the three related topics: the paraxial approximation, the absorbing boundary conditions and domain decomposition. We summarize these in the next subsection.

4.5 Links between paraxial operators, absorbing boundary conditions and optimal domain decomposition algorithms

We start with the wave equation in the plane

$$\frac{1}{c^2}\frac{\partial^2 u}{\partial t^2} - \Delta u = 0, \quad \text{in} \quad \mathbb{R}^2 \times (0,T).$$

We introduce a rational function $R(ik_1, i\omega) = r(k_1/\omega)$ and the problems:

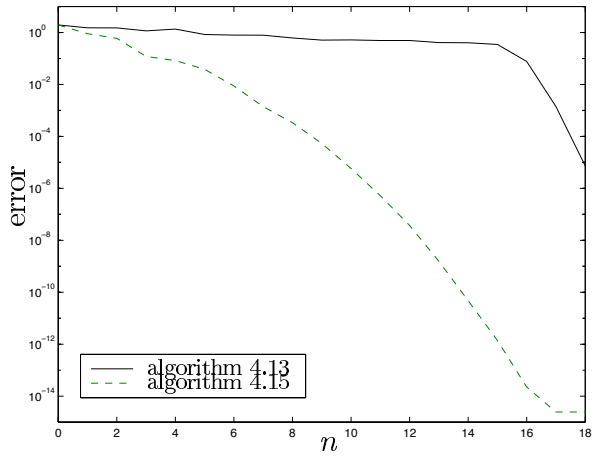

Figure 35: Convergence of the algorithm with transmission conditions (4.13) and (4.15).

(i) *The paraxial equation in the $x_2 > 0$ direction:*

$$\partial_{x_2} u + R(\partial_t, \partial_{x_1}) u = 0 \quad \text{in} \quad \mathbb{R}^2 \times (0,T)$$

(ii) *The absorbing boundary conditions:*

$$\frac{1}{c^2}\frac{\partial^2 u}{\partial t^2} - \Delta u = f \quad \text{in} \quad \mathbb{R}^2_- \times (0,T),$$
$$\partial_{x_2} u + R(\partial_t, \partial_{x_1}) u = 0, \quad x_2 = 0$$

(iii) *The domain decomposition algorithm without overlap:*

$$\left(\frac{1}{c^2}\frac{\partial^2}{\partial t^2} - \Delta\right) u_1^{n+1} = f \text{ in } \mathbb{R}^2_- \times (0,T), \quad \left(\frac{1}{c^2}\frac{\partial^2}{\partial t^2} - \Delta\right) u_2^{n+1} = f \text{ in } \mathbb{R}^2_+ \times (0,T),$$
$$(\partial_{x_2} + R(\partial_t, \partial_{x_1})) u_1^{n+1} = (\partial_{x_2} + R(\partial_t, \partial_{x_1})) u_2^n; \quad x_2 = 0,$$
$$(\partial_{x_2} - R(\partial_t, \partial_{x_1})) u_2^{n+1} = (\partial_{x_2} - R(\partial_t, \partial_{x_1})) u_1^n; \quad x_2 = 0.$$

The error is measured in the three cases for x in $[0,1]$ as follows:

(i) *Paraxial equation: the error*

$$\text{err}(x) = \sqrt{1-x^2} - r(x)$$

(ii) *Absorbing boundary conditions: the reflection coefficient*

$$\frac{\sqrt{1-x^2} - r(x)}{\sqrt{1-x^2} + r(x)}$$

(iii) *Domain decomposition algorithm: the convergence rate*

$$\frac{\sqrt{1-x^2} - r(x)}{\sqrt{1-x^2} + r(x)}$$

5 Classical layers and perfectly matched layers for hyperbolic problems

The layer or sponge methods consist of surrounding the domain of interest by a layer. This layer should be designed in such a way that it produces as low reflection as possible and the waves are absorbed in the layer. Furthermore, to save computation, it should be made thin.

In practice, defining the layer can be very involved as it depends very much on the frequency of the incoming signal. This explains why layer methods have not been very much used. More evolved models have been proposed (coupling layers and absorbing boundary conditions) [24], but the increase in complexity lessens the interest of these methods.

Bérenger's work [7] has renewed the interest in these layer methods; the Bérenger perfectly matched layer, PML, has many attractive features: it absorbs waves of any wavelength and any frequency without spurious reflection; moreover, the corner problem is easily solved by a wise choice of the layer parameters. Finally, it is very easy to integrate into an existing code. Unfortunately, as applied to the Maxwell system, the original method leads to a system which has lost the most important properties of the Maxwell system: strong hyperbolicity and symmetry.

In the last part of this section we propose an algebraic technique leading to a new PML model which is strongly well-posed and preserves the symmetry. We start however with the classical methods.

5.1 The classical layers

The layers techniques are often inspired by well-known physical models (soundproof rooms of acoustics laboratories). As an example, we first present some models for the wave equation in two dimensions. These examples, although simple, highlight the power and the limitations of the classical approach. We summarize here some of the results by M. Israeli and S. Orszag in [24].

We consider the wave equation in two dimensions:

$$\frac{\partial^2 u}{\partial t^2} - \Delta u = 0.$$

A simple model can be obtained by adding a friction term

$$\frac{\partial^2 u}{\partial t^2} + \sigma(x)\frac{\partial u}{\partial t} - \Delta u = 0,$$

where σ is a positive function of x. In such a medium the energy is decreasing: it is a lossy medium.

More precisely, we consider the case of a propagation in the half-space $x_1 < 0$, and we build the layer of width δ on the right of the domain

$$\begin{cases} \dfrac{\partial^2 u}{\partial t^2} + \sigma(x)\dfrac{\partial u}{\partial t} - \Delta u = 0, \quad (x_1, x_2) \in (-\infty, \delta) \times \mathbb{R} \\ u(0,\cdot) = u^{(0)}, \quad \dfrac{\partial u}{\partial t}(0,\cdot) = u^{(1)} \\ u(\delta, x_2, t) = 0 \end{cases} \tag{5.1}$$

with $\sigma(x) = 0$ for $x_1 < 0$. The initial data are supported in $\mathbb{R}^2_-$.

The choice of the damping factor σ is crucial. First, the reflection at the boundary of the layer must be maintained as small as possible. Second, the decay in the layer must be sufficiently significant so that the Dirichlet condition imposed on the exterior boundary of the layer does not produce reflection. The plane wave analysis gives a more precise idea of the best choice of the damping factor.

We call u^- the solution in $\mathbb{R}^2_-$ and u^+ the solution in $]0, \delta[\times\mathbb{R}$. They are given by

$$u^- = e^{i(k_1x_1+k_2x_2-\omega t)} + Re^{i(-k_1x_1+k_2x_2-\omega t)},$$
$$u^+ = T_1e^{i(k_1^\sigma x_1+k_2x_2-\omega t)} + T_2e^{i(-k_1^\sigma x_1+k_2x_2-\omega t)}.$$

The dispersion relations are

$$k_1^2 + k_2^2 = \omega^2, \qquad (k_1^\sigma)^2 = k_1^2 + i\omega\sigma;$$

k_1 and k_1^σ are defined by

$$\frac{k_1}{\omega} > 0; \quad k_1^\sigma \in \mathbb{C}, \quad \frac{\Re k_1^\sigma}{\omega} > 0,$$

such that $e^{i(k_1x_1+k_2x_2-\omega t)}$ and $e^{i(k_1^\sigma x_1+k_2x_2-\omega t)}$ propagate to the left. For any ω the imaginary part of k_1^σ is positive, and we have the following process: the incident wave $u^I = e^{i(k_1x_1+k_2x_2-\omega t)}$ reflects at $x_1 = 0$ into $R_0e^{i(-k_1x_1+k_2x_2-\omega t)}$ and transmits in the layer into $T_0e^{i(k_1^\sigma x_1+k_2x_2-\omega t)}$. This wave is in turn reflected at the end of the layer $x_1 = \delta$ into $R_\delta T_0e^{i(-k_1^\sigma x_1+k_2x_2-\omega t)}$ and then reflected, and so on for ever. The coefficients are given by

$$R_0 = \frac{k_1 - k_1^\sigma}{k_1 + k_1^\sigma}, \qquad T_0 = 1 + R_0, \qquad R_\delta = -e^{2ik_1^\sigma\delta}.$$

For the full process, the coefficients are given by

$$R = \frac{R_0 + R_\delta}{1 + R_0R_\delta}, \qquad T_1 = \frac{1+R}{1+R_\delta}, \qquad T_2 = R_\delta T_1.$$

It is easy to see that if σ is large then $|R_0|$ is close to 1. On the other hand, if σ is small, $|R_0|$ is small and R_δ is close to 1, unless δ is large. The tuning of the coefficients is thus difficult. Other attempts have been made to improve the results: adding a term $-\mu(x)\partial^3u/\partial t\partial x_1^2$, or replacing the term $\partial u/\partial t$ by $\partial u/\partial t + \partial u/\partial x_1$[24]. In the latter case, the reflection coefficient is small for low angles of incidence which considerably improves the results and has made this strategy attractive. However, the breakthrough came later with the PML we describe now.

5.2 The PML approach of Bérenger

In the mid-90s, Bérenger [7] proposed a new layer method for Maxwell's equation, namely the *perfectly matched layer* or PML. The strength of this new method is that the layer absorbs waves regardless of their frequency and angle of incidence.

For simplicity we describe the method for the two-dimensional Maxwell equations in the transverse electric mode (TE), although all the developments in [7] have been made in the

three-dimensional case. The Maxwell system then has only three unknowns, (E_1, E_2, H_3), related as follows:

$$\begin{cases} \epsilon\dfrac{\partial E_1}{\partial t} + \sigma E_1 - \dfrac{\partial H_3}{\partial x_2} = 0, \\ \epsilon\dfrac{\partial E_2}{\partial t} + \sigma E_2 + \dfrac{\partial H_3}{\partial x_1} = 0, \\ \mu\dfrac{\partial H_3}{\partial t} + \sigma^* H_3 + \dfrac{\partial E_2}{\partial x_1} - \dfrac{\partial E_1}{\partial x_2} = 0. \end{cases} \tag{5.2}$$

The coefficients ϵ and μ are the permittivity and permeability of the medium, σ is the electric conductivity and σ^* the magnetic conductivity. To establish a PML model in the region $\Omega_+ = \{x_1 > 0\}$, we split the magnetic field into two non-physical subcomponents $H_3 = H_{31} + H_{32}$, and we introduce damping factors σ_i and σ_i^*, for $i = 1, 2$, with $\sigma_1 = \sigma_2 = \sigma$ and $\sigma_1^* = \sigma_2^* = \sigma^*$ in $\Omega_- = \mathbb{R}^2 - \Omega_+$ (the domain of interest).

We then write a modified version of (5.2) in a form where only one spatial derivative appears in each equation:

$$\begin{cases} \epsilon\dfrac{\partial E_1}{\partial t} + \sigma_2 E_1 - \dfrac{\partial (H_{31} + H_{32})}{\partial x_2} = 0, \\ \epsilon\dfrac{\partial E_y}{\partial t} + \sigma_1 E_2 + \dfrac{\partial (H_{31} + H_{32})}{\partial x_1} = 0, \\ \mu\dfrac{\partial H_{31}}{\partial t} + \sigma_1^* H_{31} + \dfrac{\partial E_2}{\partial x_1} = 0, \\ \mu\dfrac{\partial H_{32}}{\partial t} + \sigma_2^* H_{32} - \dfrac{\partial E_1}{\partial x_2} = 0. \end{cases} \tag{5.3}$$

The Bérenger medium is characterized by the fictitious conductivities. We call the system $\mathbf{PML}(\sigma_1, \sigma_1^*, \sigma_2, \sigma_2^*)$. The Maxwell system appears as a particular case of the PML equations. It corresponds to $\mathbf{PML}(\sigma, \sigma^*, \sigma, \sigma^*)$:

$$\begin{aligned} \mathbf{PML}(\sigma, \sigma^*, \sigma, \sigma^*) &\longrightarrow \text{absorbing medium}, \\ \mathbf{PML}(0, 0, 0, 0) &\longrightarrow \text{vacuum}. \end{aligned}$$

5.1 Remark The original equations are recovered by adding the equations for the split fields.

We describe now the important features of this model [7]. Suppose the conductivities satisfy the *matching conditions*

$$\frac{\sigma_i}{\epsilon} = \frac{\sigma_i^*}{\mu}, \tag{5.4}$$

Then for harmonic fields, the amplitudes decays exponentially. They are of the form

$$\Psi \exp\left(i\omega\left(t - \frac{1}{c}\boldsymbol{x}\cdot\boldsymbol{C}\right)\right)\exp\left(-\frac{\sigma_1 C_1}{\epsilon c}x_1\right)\exp\left(-\frac{\sigma_2 C_2}{\epsilon c}x_2\right)$$

where c is the speed of light, $c = 1/\sqrt{\epsilon\mu}$, and $\boldsymbol{C}$ is the unitary wave vector, $\boldsymbol{C} = (\cos\theta, \sin\theta)$.

Consider now two PML media $\mathbf{PML}(\sigma_1^1, \sigma_1^{1*}, \sigma_2^1, \sigma_2^{1*})$ and $\mathbf{PML}(\sigma_1^2, \sigma_1^{2*}, \sigma_2^2, \sigma_2^{2*})$. The reflection coefficient between these media vanishes provided

(i) *their conductivities satisfy the matching conditions* (5.4)*;*

(ii) $\Sigma^1 \cdot \tau = \Sigma^2 \cdot \tau$ *with* $\Sigma = (\sigma_1, \sigma_2)$ *and* τ *is tangent to the interface.*

These results lead to the now famous diagram 36 extracted from [7] which provides the complete strategy for PML, including the question of corners, which has never been satisfactorily solved for absorbing boundary conditions :

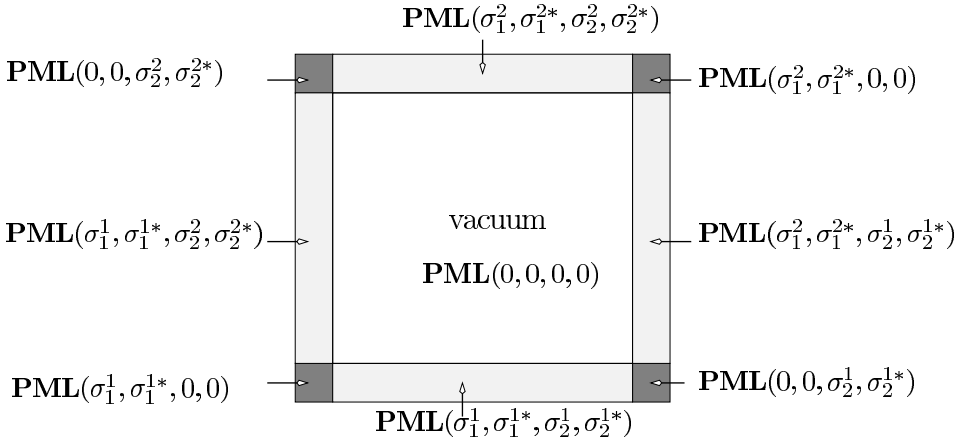

Figure 36: The **PML** technique [7].

In the harmonic case, the model **PML**$(\sigma, \sigma, 0, 0)$ becomes:

$$\begin{cases} i\epsilon\omega\hat{E}_1 - \dfrac{\partial(\hat{H}_{31} + \hat{H}_{32})}{\partial x_2} = 0, \\ i\epsilon\omega\hat{E}_2 + \sigma\hat{E}_2 + \dfrac{\partial(\hat{H}_{31} + \hat{H}_{32})}{\partial x_1} = 0, \\ i\mu\omega\hat{H}_{31} + \sigma\hat{H}_{31} + \dfrac{\partial\hat{E}_2}{\partial x_1} = 0, \\ i\mu\omega\hat{H}_{32} - \dfrac{\partial\hat{E}_1}{\partial x_2} = 0. \end{cases} \tag{5.5}$$

We can add the last two equations and keep only one unknown $\hat{H}_3 = \hat{H}_{31} + \hat{H}_{32}$:

$$\frac{i\omega}{i\omega\mu + \sigma(x)} \frac{\partial}{\partial x_1} \left(\frac{i\omega}{i\omega\epsilon + \sigma(x)} \frac{\partial}{\partial x_1} \hat{H}_3 \right) + c^2 \frac{\partial^2}{\partial x_2^2} \hat{H}_3 + \omega^2 \hat{H}_3 = 0.$$

In [10], Collino and Monk show that this problem is well posed except for a discrete set of exceptional frequencies (which may be empty), and that the PML formulation amounts to the continuation of the Green's function into the complex plane. As a matter of fact, making the complex change of variables

$$x_1' = x_1 - \frac{i}{\omega} \int_0^{x_1} \sigma(\xi)\, d\xi,$$

we retrieve the Helmholtz equation, so that the PML model can be viewed as a complex change of variables applied to the original system [34].

More generally, we consider a general first order system written in the form

$$\frac{\partial \varphi}{\partial t} + A_1 \frac{\partial \varphi}{\partial x_1} + A_2 \frac{\partial \varphi}{\partial x_2} = 0, \tag{5.6}$$

where φ lives in $\mathbb{R}^N$. In order to obtain the PML model we split the unknown φ into two non-physical parts $\varphi = \varphi_1 + \varphi_2$, and we write the system in a form where only one spatial derivation appears in each equation:

$$\begin{cases} \dfrac{\partial \varphi_1}{\partial t} + A_1 \dfrac{\partial \varphi}{\partial x_1} = 0, \\ \dfrac{\partial \varphi_2}{\partial t} + A_2 \dfrac{\partial \varphi}{\partial x_2} = 0, \end{cases}$$

then we introduce damping factors $\sigma_1(x_1)$ and $\sigma_2(x_2)$, and the PML system becomes :

$$\begin{cases} \dfrac{\partial \varphi_1}{\partial t} + A_1 \dfrac{\partial \varphi}{\partial x_1} + \sigma_1(x_1)\varphi_1 = 0, \\ \dfrac{\partial \varphi_2}{\partial t} + A_2 \dfrac{\partial \varphi}{\partial x_2} + \sigma_2(x_2)\varphi_2 = 0, \\ \varphi = \varphi_1 + \varphi_2. \end{cases} \tag{5.7}$$

5.2.1 Propagation properties

We start with the propagation in free space. From a plane wave solution of the original system (5.6), we can construct a plane wave solution of (5.7). To this end let

$$\mathbf{\Phi} = \mathbf{\Phi_0} e^{i(\boldsymbol{k}\cdot\boldsymbol{x} - \omega t)}$$

be a solution of (5.6). Then we obtain a solution of (5.7) as

$$\boldsymbol{\varphi}_i = \boldsymbol{\alpha}_i e^{i(\boldsymbol{k}\cdot\tilde{\boldsymbol{x}}(\boldsymbol{x}) - \omega t)}$$

with

$$\tilde{x}_j = \int_0^{x_j} \left(1 - \frac{i\sigma_j(\xi)}{\omega}\right) d\xi \tag{5.8}$$

and

$$\boldsymbol{\alpha}_i = \frac{k_i}{\omega} A_i \mathbf{\Phi_0}.$$

Thus if σ_i is chosen such that it vanishes in the domain of interest, and is strictly positive in the layer wich is orthogonal to x_i, the plane wave solutions of (5.7) coincide with those of the original system (5.6) in the domain of interest, and the amplitude of the wave is exponentially decaying in the layer.

Consider now a PML of thickness δ orthogonal to the x_1-direction. Imposing a homogeneous Dirichlet condition $\varphi_j = 0$ at the external boundary of the PML (at $x_1 = \delta$) and writing $\varphi_{j,\text{inc}} + R\varphi_{j,\text{ref}} = 0$ at $x_1 = \delta$, we find the amplitude of the reflected wave

$$R = -\exp\left(-2ik_1 \int_0^{\delta} \left(1 - \frac{i\sigma_1(\xi)}{\omega}\right) d\xi\right).$$

Since $k_1/\omega > 0$, the reflection coefficient is exponentially small and it can be made as small as desired by increasing the thickness of the layer; in the numerical application it is necessary to find a good compromise between the thickness of the layer and the "acceptable" error.

5.2.2 Well-posedness

The time-domain PML model is mainly designed for propagation models, i.e. hyperbolic equations. In this respect, Bérenger's approach presents some inconveniences: even if the original model is strongly well-posed, the PML model becomes weakly well-posed. This is the case for most systems, which are in fact symmetric, as for instance the Maxwell system, the Euler system, the wave equation and the elastodynamics system. The weak well-posedness can generate instabilities in the numerical schemes, and spurious reflection at the external boundary. The loss of symmetry is a disadvantage for storage reasons.

To make these notions more precise (for details see [26]), let $P(\partial/\partial x)$ be a constant-coefficient operator. We introduce the Cauchy problem:

$$\begin{cases} \varphi_t - P(\partial/\partial x)\varphi = 0 \\ \varphi(x,0) = \varphi_0(x). \end{cases} \tag{5.9}$$

We make the following definitions:

(1) Problem (5.9) is *strongly well-posed* if there is a real number α and a positive real number K such that for any smooth initial data we have

$$\|\varphi(.,t)\|_{L^2} \leq Ke^{\alpha t}\|\varphi_0\|_{L^2}, \quad t \geq 0.$$

(2) Problem (5.9) is *weakly well-posed* if there is a strictly positive q, a real number α and a positive real number K such that for any smooth initial data

$$\|\varphi(.,t)\|_{L^2} \leq Ke^{\alpha t}\|\varphi_0\|_{H^q}, \quad t \geq 0.$$

There is an algebraic criterium for this definition of well-posedness. Let q be a positive integer and α a real number. The following conditions are equivalent:

(i) There is $K_1 > 0$ such that

$$|e^{P(i\omega)t}| \leq K_1(1+|\omega|^q)e^{\alpha t}, \quad \omega \in \mathbb{R}^n,\ t \geq 0;$$

(ii) There is K_2 such that

$$\|\varphi(.,t)\|_{L^2} \leq K_2 e^{\alpha t}\|\varphi_0\|_{H^q}, \quad t \geq 0$$

for all φ_0 sufficiently smooth.

Suppose now the operator P to be of first order in space, $P(\partial/\partial x) = \sum_{j=1}^n A_j \partial/\partial x_j$. We define the symbol $P(i\zeta) = i\sum_{j=1}^n \zeta_j A_j$. System (5.9)) is called:

(i) *weakly hyperbolic* if for any ζ in $\mathbb{R}^N$ the eigenvalues of $P(i\zeta)$ are purely imaginary;

(ii) *strongly hyperbolic* if for any ζ in $\mathbb{R}^N$, $|\zeta| = 1$, the eigenvalues of $P(i\zeta)$ are purely imaginary, and furthermore there is a uniform transformation to diagonal form;

(iii) *symmetric hyperbolic* if $A_j = A_j^*$ for any j;

(iv) *strictly hyperbolic* if for any ζ in $\mathbb{R}^N$, $\zeta \neq 0$, the eigenvalues of $P(i\zeta)$ are purely imaginary and distinct.

We have the following relations between well-posedness and hyperbolicity:

(i) strongly hyperbolic $\iff$ strongly well-posed;

(ii) weakly hyperbolic $\iff$ weakly well-posed;

(iii) symmetric hyperbolic $\Longrightarrow$ strongly hyperbolic $\Longrightarrow$ strongly well-posed;

(iv) strictly hyperbolic $\Longrightarrow$ strongly hyperbolic $\Longrightarrow$ strongly well-posed.

As an example, the Maxwell system in general and the (TE) system (5.2) in particular are symmetric hyperbolic. The eigenvalues are simple: 0, $\pm i|\zeta|$. However, the Bérenger system (5.3) is not symmetric nor even strongly well-posed: 0 is a double eigenvalue, and the dimension of the corresponding eigenspace is still 1. This inconvenience is inherent in the decomposition. One can prove for this system that if (φ_1, φ_2) is a solution of the related Cauchy problem, then

$$||(\varphi_1, \varphi_2)||_{L^2} \leq Ce^{\alpha t}||(\varphi_1, \varphi_2)(0, \cdot)||_{H^1}.$$

Moreover, this estimate is optimal [33].

5.2.3 Some examples

The Bérenger technique has been used for various hyperbolic problems [33, 32, 31, 30, 3, 2]. We focus here on the two-dimensional Euler system. The compressible Euler system linearized at constant flow $(\boldsymbol{U}, R = c^2)$ can be written as a symmetric system

$$\frac{\partial \varphi}{\partial t} + \sum_{j=1}^{2} A_j \frac{\partial \varphi}{\partial x_j} = 0$$

with

$$\varphi = \begin{pmatrix} u_1 \\ u_2 \\ \rho \end{pmatrix}, \qquad A_1 = \begin{pmatrix} U_1 & 0 & c \\ 0 & U_1 & 0 \\ c & 0 & U_1 \end{pmatrix}, \qquad A_2 = \begin{pmatrix} U_2 & 0 & 0 \\ 0 & U_2 & c \\ 0 & c & U_2 \end{pmatrix}.$$

We shall consider in the sequel the case where the linearization is made about velocity 0. For the general case, a change of variables along the flow produces moving PMLs [33, 2]. The simplest strategy is to split the density into $\rho = \rho_1 + \rho_2$, and then the continuity equation becomes:

$$\frac{\partial \rho_i}{\partial t} + c\frac{\partial u_i}{\partial x_i} = 0, \quad i = 1, 2.$$

Next, we introduce the damping factor $\sigma(x)$, with $\sigma(x) > 0$ in the PML region $\{x_1 > 0\}$, and zero elsewhere. The PML model is then given by

$$\begin{cases} \dfrac{\partial \rho_1}{\partial t} + \sigma(x)\rho_1 + c\dfrac{\partial u_1}{\partial x_1} = 0 \\ \dfrac{\partial \rho_2}{\partial t} + c\dfrac{\partial u_2}{\partial x_2} = 0 \\ \dfrac{\partial u_1}{\partial t} + \sigma(x)u_1 + c\dfrac{\partial \rho}{\partial x_1} = 0 \\ \dfrac{\partial u_2}{\partial t} + c\dfrac{\partial \rho}{\partial x_2} = 0 \end{cases} \tag{5.10}$$

Again, this problem is only weakly well-posed. We introduce now a new model, based on (5.10), which will be symmetric hyperbolic and thus strongly well-posed.

5.2 Remark For the wave equation

$$\frac{\partial^2 \rho}{\partial t^2} - \Delta \rho = 0,$$

we write the problem as a first order hyperbolic system using the Euler form, and we proceed as before [32]. Another approach, used in [10], is based on the complex change of variables (5.8) and a fast Fourier transform.

5.3 Remark For the system of isotropic elastodynamics in two dimensions, one can obtain Berenger-type PMLs as well [11]. The difficulty comes for anisotropic behaviors.

5.3 A well-posed PML model

Various improvements of PML models have been proposed to circumvent the problems mentioned in the previous section; in [21] and [2], the authors (following the approach developed for electromagnetism in [1]) modify the Euler equations by introducing low-order terms only. Thus by construction the resulting model is strongly well-posed. We describe here an algebraic technique leading to a new PML model in the primitive variables, which is symmetric and preserves the propagation and absorption advantages of the Berenger model [31]. This model is similar to the one obtained in [21]. However, the approaches are different since we start from Bérenger's model.

We consider the general harmonic PML model in the frequency domain

$$\begin{cases} (i\omega + \sigma_1(x_1))\hat{\varphi}_1 + A_1\dfrac{\partial \hat{\varphi}}{\partial x_1} = 0 \\ (i\omega + \sigma_2(x_2))\hat{\varphi}_2 + A_2\dfrac{\partial \hat{\varphi}}{\partial x_2} = 0. \end{cases}$$

Adding these equations, we retrieve the physical unknowns

$$i\omega\hat{\varphi} + \left(S_1 A_1 \frac{\partial \hat{\varphi}}{\partial x_1} + S_2 A_2 \frac{\partial \hat{\varphi}}{\partial x_2}\right) = 0, \tag{5.11}$$

with $S_i = i\omega/(i\omega + \sigma_i(x_i))$.

A PML medium is thus characterized by (S_1, S_2) or (σ_1, σ_2) . Here the matching conditions of Bérenger are assumed from the beginning. One can prove that by choosing σ_1 and σ_2 as in Fig. 36, one can ensure the exponential decay in the layer, and no reflection occurs between two layers.

In order to retrieve a well-posed PML model in the time-domain, we make a change of basis in the spatial operator $\sum S_i A_i \partial/\partial x_i$ which relies on an algebraic lemma:

5.4 Lemma *There exist two invertible operators M and N such that*

$$S_1 A_1 \frac{\partial}{\partial x_1} + S_2 A_2 \frac{\partial}{\partial x_2} = M \left(A_1 \frac{\partial}{\partial x_1} + A_2 \frac{\partial}{\partial x_2} \right) N \tag{5.12}$$

which satisfy

$$A_1 \frac{\partial}{\partial x_1} N + A_2 \frac{\partial}{\partial x_2} N = 0 \quad \textit{and} \quad \lim_{\sigma_1, \sigma_2 \to 0} N = I. \tag{5.13}$$

Proof The proof is constructive. We first seek invertible operators M and N such that

$$\begin{aligned} M A_1 N - S_1 A_1 &= 0 \\ M A_2 N - S_2 A_2 &= 0. \end{aligned} \tag{5.14}$$

Using the special form of the matrices A_i, we find the general form of M and N solving (5.14) to be:

$$N = \begin{pmatrix} S_1 S_2^{-1} \lambda & 0 & n_{13} \\ 0 & \lambda & n_{23} \\ 0 & 0 & n_{33} \end{pmatrix}, \qquad M = \begin{pmatrix} \dfrac{S_1}{n_{33}} & 0 & 0 \\ 0 & \dfrac{S_2}{n_{33}} & 0 \\ -\dfrac{n_{13} S_2}{\lambda n_{33}} & -\dfrac{n_{23} S_2}{\lambda n_{33}} & \dfrac{S_2}{\lambda} \end{pmatrix},$$

where n_{13}, n_{23}, n_{33} are free parameters. We now choose N as simple as possible:

$$N = \begin{pmatrix} S_2^{-1} & 0 & 0 \\ 0 & S_1^{-1} & 0 \\ 0 & 0 & 1 \end{pmatrix}, \qquad M = \begin{pmatrix} S_1 & 0 & 0 \\ 0 & S_2 & 0 \\ 0 & 0 & S_1 S_2 \end{pmatrix},$$

and since S_i depends only on x_i, (5.13) is satisfied. □

With the above lemma, (5.11) becomes

$$i\omega \hat{\varphi} + M \left(A_1 \frac{\partial}{\partial x_1} + A_2 \frac{\partial}{\partial x_2} \right) (N \hat{\varphi}) = 0,$$

and the change of unknowns $\tilde{\varphi} = N\varphi$ gives

$$i\omega M^{-1} N^{-1} \widehat{\tilde{\varphi}} + \left(A_1 \frac{\partial}{\partial x_1} + A_2 \frac{\partial}{\partial x_2} \right) \widehat{\tilde{\varphi}} = 0.$$

In order to establish the time-domain model, we start by writing the operator $i\omega M^{-1}N^{-1}$ in the form:

$$i\omega M^{-1}N^{-1} = i\omega I + C + R(U_\omega)^{-1}$$

with

$$C = \begin{pmatrix} \sigma_1-\sigma_2 & 0 & 0 \\ 0 & \sigma_2-\sigma_1 & 0 \\ 0 & 0 & \sigma_1+\sigma_2 \end{pmatrix}, \qquad R = \begin{pmatrix} \sigma_2(\sigma_2-\sigma_1) & 0 & 0 \\ 0 & \sigma_1(\sigma_1-\sigma_2) & 0 \\ 0 & 0 & \sigma_1\sigma_2 \end{pmatrix},$$

$$U_\omega = \begin{pmatrix} (i\omega+\sigma_2) & 0 & 0 \\ 0 & (i\omega+\sigma_1) & 0 \\ 0 & 0 & i\omega \end{pmatrix}.$$

Finally the time-harmonic model is reduced to

$$i\omega\widehat{\tilde{\varphi}} + C\widehat{\tilde{\varphi}} + R(U_\omega)^{-1}\widehat{\tilde{\varphi}} + \left(A_1\frac{\partial}{\partial x_1} + A_2\frac{\partial}{\partial x_2}\right)\widehat{\tilde{\varphi}} = 0. \tag{5.15}$$

5.5 Remark The new unknown $\tilde{\varphi}$ is equal to the original one, φ, in the domain of interest (i.e. when $\sigma_1 = \sigma_2 = 0$). Moreover, when transmitted to the PML the new unknown $\tilde{\varphi}$ does not "see" a contrast between the two mediums (due to $\lim_{\sigma_1,\sigma_2\to 0} N = I$).

Finally, this change of unknowns can be interpreted as a complex change of basis ($S_1 A = MAN$), thus generalizing the change of variables in [34].

By an inverse Fourier transform of (5.15), we would obtain a model which is not local in time. Instead, we increase the number of unknowns (which is a classical technique when studying dispersive materials [36]) and introduce a new vector-valued variable $\tilde{\psi}$ such that $U_\omega\widehat{\tilde{\psi}} = \widehat{\tilde{\varphi}}$. Back to the time domain we obtain

$$\begin{cases} \dfrac{\partial\tilde{\varphi}}{\partial t} + C\tilde{\varphi} + R\,\tilde{\psi} + \left(A_1\dfrac{\partial}{\partial x_1} + A_2\dfrac{\partial}{\partial x_2}\right)\tilde{\varphi} = 0, \\ \dfrac{\partial\tilde{\psi}}{\partial t} + D\tilde{\psi} - \tilde{\varphi} = 0, \\ \tilde{\psi}(0,\cdot) = 0, \end{cases}$$

with

$$D = \begin{pmatrix} \sigma_2 & 0 & 0 \\ 0 & \sigma_1 & 0 \\ 0 & 0 & 0 \end{pmatrix}$$

or

$$\frac{\partial\Phi}{\partial t} + \left(\mathcal{C} + \mathcal{A}\left(\frac{\partial}{\partial x_1}, \frac{\partial}{\partial x_2}\right)\right)\Phi = 0 \tag{5.16}$$

where we have set

$$\Phi = \begin{pmatrix} \tilde{\varphi} \\ \tilde{\psi} \end{pmatrix}, \quad \mathcal{C} = \begin{pmatrix} C & R \\ -I & D \end{pmatrix} \quad \text{and} \quad \mathcal{A}\left(\frac{\partial}{\partial x_1}, \frac{\partial}{\partial x_2}\right) = \begin{pmatrix} A_1\dfrac{\partial}{\partial x_1} + A_2\dfrac{\partial}{\partial x_2} & 0 \\ 0 & 0 \end{pmatrix} \tag{5.17}$$

This model preserves the absorption and decay properties of the Bérenger model. Furthermore, it is hyperbolic symmetric, as shown by (5.16), (5.17). We summarize.

5.6 Theorem *The model given by* (5.16), (5.17) *is a* PML *model for the linearized Euler equations. Moreover, the Cauchy problem associated to this model is strongly well-posed.*

5.7 Remark For a layer starting at $x_1 = 0$, if we choose σ_1 to be a constant (non-zero) in the layer, the model is no longer perfectly matched. Indeed, in this case we cannot simultaneously ensure the continuity of all fields since for this we must have $\sigma_1(0) = 0$. In practice it is preferable to choose a damping factor σ_1 which does not become rapidly significant (for example parabolic). This remark is also valid for all layer methods.

5.4 Numerical results

To verify the efficiency of our PML model, we present numerical results on a benchmark problem in computational aeroacoustics [21, 23]. The initial condition is in the isentropic case an acoustic pulse centered at point x_a,

$$P_0 = \rho_0 = \exp\left(-(\ln 2)\frac{|x - x_a|^2}{9}\right), \qquad u_0 = v_0 = 0.$$

The computational domain is $[-60, 60] \times [-60, 60]$, the domain of interest is $[-50, 50] \times [-50, 50]$ surrounded by a layer of thickness $N = 10$. The damping factors $\sigma_i(x_i)$ are chosen as $\sigma_i(x_i) = \sigma_0(d_i(x_i)/D_i)^3$, where D_i is the thickness of the layer in the x_i-direction and $d_i(x_i)$ is the distance from the interface to the point in the layer. According to the results observed in [23], we take $\sigma_0 D/N \cong 8$.

The scheme is fourth order Runge-Kutta in time, and a seven point finite difference scheme in space. The contour plots of the pressure p are shown for several times in Fig. 37. We can see that the field is well absorbed by the PML layer (the wave arrives at $t = 30$ in the PML) with no noticeable reflection. The Dirichlet condition imposed on the exterior boundary of the PML does not generate spurious reflection, and the wave is totally absorbed after $t = 100$.

5.5 Conclusion

The methods developed in this section are a very promising alternative to absorbing boundary conditions for linear hyperbolic problems with constant coefficients. Progress needs to be made for more complicated models, as for instance Euler models with non-constant mean flows, or anisotropic elasticity models, and of course non-linear problems.

Acknowlegments The authors are very grateful to Martin Gander for his invitation to Montreal and his contribution to this work.

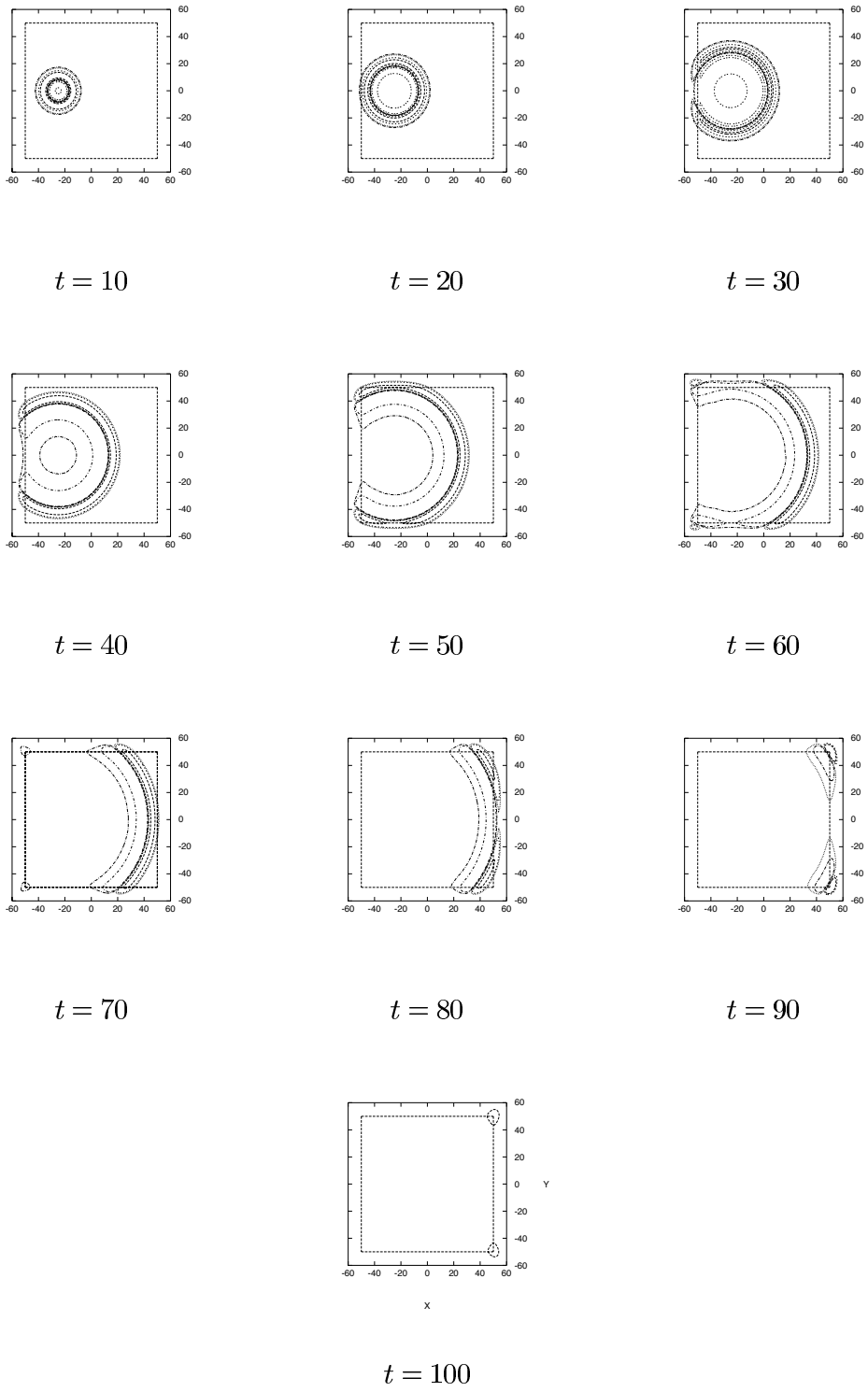

Figure 37: Pressure contours for the new PML model from [33].

References

[1] S. Abarbanel and D. Gottlieb, A mathematical analysis of the PML method, *J. Comput. Phys.* **134** (1997), 357–363.

[2] S. Abarbanel, D. Gottlieb, and S. Hesthaven, Well-posed perfectly matched layers for advective acoustics, *J. Comput. Phys.* **154** (1999), 266–283.

[3] A. Bah, Sur la modélisation de milieux fictifs absorbants de type couche de Bérenger, Ph.D. thesis, Université de Toulouse, 2001.

[4] A. Bamberger, B. Engquist, L. Halpern, and P. Joly, Higher order wave equation approximation in heterogenous media, *SIAM J. Appl. Math.* **48** (1) (1988), 129–154.

[5] A. Bayliss and E. Turkel, Radiation boundary conditions for wave-like equations, *Comm. Pure Appl. Math.* **33** (1980), 707–725.

[6] E. Bécache, F. Collino, and P. Joly, Higher-order variational finite difference schemes for solving 3-d paraxial wave equations using splitting techniques, *Wave Motion* **31** (2) (2000), 101–116.

[7] J. P. Bérenger, Three-dimensional perfectly matched layer for the absorption of electromagnetic waves, *J. Comput. Phys.* **114** (1994), 185–200.

[8] R. W. Clayton and B. Engquist, Absorbing boundary conditions for acoustic and elastic wave equations, *Bull. Seismic Soc. America* **67** (6) (1977), 1529–1540.

[9] R. W. Clayton and B. Engquist, Absorbing boundary conditions for wave equation migration, *Geophysics* **45** (5) (1980), 895–904.

[10] F. Collino and P. Monk, The perfectly matched layer in curvilinear coordinates, *SIAM J. Sci. Comput.* **19** (6) (1998), 2061–2090.

[11] F. Collino and C. Tsogka, Application of the PML absorbing layer model to the linear elastodynamic problem in anisotropic heteregenous media, Technical Rep. 3471, INRIA, August 1998.

[12] B. Engquist and A. Majda, Absorbing boundary conditions for the numerical simulation of waves, *Math. Comp.* **31** (1977), 629–651.

[13] B. Engquist and A. Majda, Radiation boundary conditions for acoustic and elastic calculations, *Comm. Pure Appl. Math.* **32** (1979), 313–357.

[14] T. Gallouet, R. Herbin, and M.-H. Vignal, Error estimates for the approximate finite volume solution of convection diffusion equations with general boundary conditions, *SIAM J. Numer. Anal.* **37** (6) (2000), 1935–1972.

[15] M. J. Gander, Analysis of parallel algorithms for time dependent partial differential equations, Ph.D. thesis, Stanford University, 1997.

[16] M. J. Gander, L. Halpern, and F. Nataf, Domain decomposition methods for wave propagation, in: *Proc. Fifth Internat. Conf. on Mathematical and Numerical Aspects of Wave Propagation Phenomena*, INRIA-SIAM, 2000.

[17] M. J. Gander, L. Halpern, and F. Nataf, Optimal Schwarz waveform relaxation for the one dimensional wave equation, Internal Report 469, École Polytechnique, Palaiseau, Sept. 2001.

[18] B. Gustafsson, Numerical boundary conditions, *Lectures in Appl. Math.* **22** (1985), 279–308.

[19] L. Halpern, Absorbing boundary conditions for the discretization schemes of the one-dimensional wave equation, *Math. Comp.* **38** (158) (1982), 415–429.

[20] L. Halpern and L. Trefethen, Well-posedness of one-way wave equations and absorbing boundary conditions, *Math. Comp.* **47** (176) (1986), 421–435.

[21] J. S. Hesthaven, On the analysi s and construction of perfectly matched layers for the linearized Euler equations, *J. Comput. Phys.* **142** (1) (1998), 129–147.

[22] R. Higdon, Initial-boundary value problems for linear hyperbolic systems, *SIAM Rev.* **28** (2) (1986), 177–217.

[23] F. Hu, On absorbing boundary conditions for linearized Euler equations by a perfectly matched layer, *J. Comput. Phys.* **129** (1996), 201–219.

[24] M. Israeli and S. Orszag, Approximation of radiation boundary conditions, *J. Comput. Phys.* **41** (1981), 115–135.

[25] C. Japhet, F. Nataf, and F. Rogier, The optimized order 2 method. Application to convection-diffusion problems, *Future Generation Computer Systems FUTURE* **18** (2001).

[26] H.-O. Kreiss and J. Lorenz, *Initial-Boundary Value Problems and the Navier-Stokes Equations*, Academic Press, New York, 1989.

[27] D. Lee, G. Botseas, and J. S. Papadakis, Finite difference solution to the parabolic wave equation, *J. Acoustic Soc. America* **70** (3) (1981), 798–799.

[28] E. Lindman, Free space boundary conditions for the time dependent wave equation, *J. Comput. Phys.* **18** (1975), 66–78.

[29] P. L. Lions, On the Schwarz alternating method. III: a variant for nonoverlapping subdomains, in: *Proc. Third International Symposium on Domain Decomposition Methods for Partial Differential Equations* (T. F. Chan, R. Glowinski, J. Périaux, and O. Widlund, eds.), SIAM, Philadelphia, PA, 1990.

[30] P. Mazet, S. Paintandre, and A. Rahmouni, Interprétation dispersive du milieu PML de Bérenger, *C. R. Acad. Sci. Paris Sér. I Math.* **327** (1998), 59–64.

[31] A. Rahmouni, Un modèle PML bien posé pour les équations d'Euler linéarisées, *C. R. Acad. Sci. Paris Sér. I Math.* **331** (2000), 159–164.

[32] A. Rahmouni, A well-posed PML model for elastodynamic, in: *Mathematical and Numerical Aspects of Wave Propagation*, SIAM, Philadelphia, PA, 2000, 916–920.

[33] A. Rahmouni, Well-posed PML models for various hyperbolic systems, Ph.D. thesis, Université Paris XIII, 2000.

[34] C. M. Rappaport, Interpreting and improving the PML absorbing boundary condition using anisotropic lossy mapping of space, *IEEE Microwave Guided Wave Letter* (1995), no. 5, 90–92.

[35] J. C. Strikwerda, *Finite Difference Schemes and Partial Differential Equations*, Chapman & Hall, 1989.

[36] A. Taflove (ed.), *Advances in Computational Electrodynamics: The Finite-Difference Time-Domain Method*, Artech House, Boston, MA, 1998.